

การออกแบบที่รวมการหาค่าเหมาะที่สุดและการควบคุมเชิงทำนายแบบจำลองสำหรับหอกลับ



นาย ฟุค ชวน แดง

# ศูนย์วิทยพัทยากร จุฬาลงกรณ์มหาวิทยาลัย

วิทยานิพนธ์นี้เป็นส่วนหนึ่งของการศึกษาตามหลักสูตรปริญญาวิศวกรรมศาสตรมหาบัณฑิต

สาขาวิชาวิศวกรรมไฟฟ้า ภาควิชาวิศวกรรมไฟฟ้า

คณะวิศวกรรมศาสตร์ จุฬาลงกรณ์มหาวิทยาลัย

ปีการศึกษา 2553

ลิขสิทธิ์ของจุฬาลงกรณ์มหาวิทยาลัย



5 2 7 0 7 1 8 0 2 1

DESIGN OF INTEGRATED REAL TIME OPTIMIZATION  
AND MODEL PREDICTIVE CONTROL FOR DISTILLATION COLUMN

Mr. Phuc Xuan Dang

ศูนย์วิทยทรัพยากร  
จุฬาลงกรณ์มหาวิทยาลัย

A Thesis Submitted in Partial Fulfillment of the Requirements  
for the Degree of Master of Engineering Program in Electrical Engineering

Department of Electrical Engineering

Faculty of Engineering

Chulalongkorn University

Academic Year 2010

Copyright of Chulalongkorn University

530890

Thesis Title                    DESIGN OF INTEGRATED REAL TIME OPTIMIZATION  
AND MODEL PREDICTIVE CONTROL FOR DISTILLATION  
COLUMN

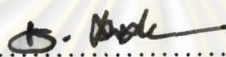
By                                    Mr. Phuc Xuan Dang

Field of Study                    Electrical Engineering

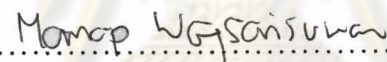
Thesis Advisor                    Associate Professor David Banjerdpongchai, Ph.D.

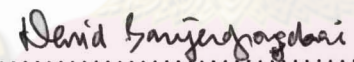
---

Accepted by the Faculty of Engineering, Chulalongkorn University in  
Partial Fulfillment of the Requirements for the Master's Degree

  
..... Dean of the Faculty of Engineering  
(Associate Professor Boonsom Lerthirunwong, Dr. Ing.)

THESIS COMMITTEE

  
..... Chairman  
(Assistant Professor Manop Wongsaisuwan, D.Eng.)

  
..... Thesis Advisor  
(Associate Professor David Banjerdpongchai, Ph.D.)

  
..... External Examiner  
(Associate Professor Waree Kongprawechnon, Ph.D.)

ศูนย์วิทยทรัพยากร  
จุฬาลงกรณ์มหาวิทยาลัย

ฟู ก ชวน แดง: การออกแบบที่รวมการหาค่าเหมาะที่สุดและการควบคุมเชิงทำนายแบบจำลองสำหรับหอกลั่น (DESIGN OF INTEGRATED REAL-TIME OPTIMIZATION AND MODEL PREDICTIVE CONTROL FOR DISTILLATION COLUMN), อ. ที่ปริกษาวิทยานิพนธ์หลัก: รศ.ดร. เดวิด บรรเจิดพงศ์ชัย, 48 หน้า.

วิทยานิพนธ์นี้นำเสนอการออกแบบที่รวมการหาค่าเหมาะที่สุดเวลาจริงกับการควบคุมเชิงทำนายแบบจำลอง พร้อมกับการประยุกต์ใช้งานกับหอกลั่น การรวมของการหาค่าเหมาะที่สุดเวลาจริงกับการควบคุมเชิงทำนายแบบจำลองแบ่งออกเป็น 2 แบบ กล่าวคือ โครงสร้าง 2 ชั้น และ โครงสร้าง 3 ชั้น ในลำดับชั้นการควบคุม ชั้นการหาค่าเหมาะที่สุดเวลาจริงจะคำนวณหาเงื่อนไขการทำงานของกระบวนการ ซึ่งอาศัยฟังก์ชันเชิงเศรษฐศาสตร์ หลังจากนั้นจุดทำงานเหมาะที่สุดจะถูกส่งไปยังชั้นการควบคุมเชิงทำนายแบบจำลอง เพื่อทำหน้าที่คุมค่าตัวแปรของกระบวนการ ณ จุดทำงานเหมาะที่สุดการควบคุมเชิงทำนายแบบจำลองอาศัยการออกแบบตัวควบคุมแบบเวลาจำกัดคือแบบจำลองปริภูมิสถานะ

วิทยานิพนธ์นี้ประกอบด้วยเนื้อหาหลัก 2 ส่วน ในส่วนแรก เรานำเสนอการออกแบบที่รวมการหาค่าเหมาะที่สุดกับการควบคุมเชิงทำนายแบบจำลองที่ระบุสำหรับหอกลั่น การออกแบบอาศัยแบบจำลองที่ระบุของหอกลั่นผลการจำลองด้วยคอมพิวเตอร์แสดงให้เห็นประสิทธิผลของวิธีการออกแบบที่นำเสนอ ในส่วนที่สอง เราขยายกรอบงานของการออกแบบเพื่อแก้ปัญหาความไม่แน่นอนของกระบวนการ ดังนั้น เรานำเสนอการออกแบบที่รวมการหาค่าเหมาะที่สุดกับการควบคุมเชิงทำนายแบบจำลองหลายแบบสำหรับหอกลั่น พลวัตของกระบวนการสอดคล้องกับเซตของแบบจำลองหลายแบบ แบบจำลองหนึ่งขึ้นอยู่กับช่วงการทำงานเฉพาะของหอกลั่นเราเปรียบเทียบผลการจำลองด้วยคอมพิวเตอร์ของการควบคุมเชิงทำนายแบบจำลองหลายแบบกับการควบคุมเชิงทำนายแบบจำลองที่ระบุ เพื่อหาข้อดีและข้อด้อยของวิธีควบคุมแต่ละวิธี

ภาควิชา วิศวกรรมไฟฟ้า  
สาขาวิชา วิศวกรรมไฟฟ้า  
ปีการศึกษา 2553

ลายมือชื่อนิสิต.....  
ลายมือชื่อ อ.ที่ปริกษาวิทยานิพนธ์หลัก.....



#5270718021: MAJOR ELECTRICAL ENGINEERING

KEYWORDS: REAL TIME OPTIMIZATION / MODEL PREDICTIVE CONTROL / MULTIPLE MODEL PREDICTIVE CONTROL / QUADRATIC PROGRAMMING / DISTILLATION COLUMN

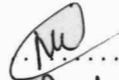
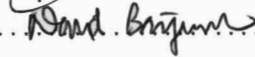
PHUC XUAN DANG: DESIGN OF INTEGRATED REAL TIME OPTIMIZATION AND MODEL PREDICTIVE CONTROL FOR DISTILLATION COLUMN  
ADVISOR: ASSOC. PROF. DAVID BANJERDPONGCHAI, Ph.D, 48 pp.

This thesis presents the design of the integrated Real Time Optimization (RTO) and Model Predictive Control (MPC) with application to distillation column. The integration of the RTO and MPC can be divided into two structures, namely, the 2-layer and 3-layer structures. In the control hierarchy, the RTO layer optimizes the plant operating conditions based on an economic function. The optimal set points of the RTO layer are transferred to the MPC layer which aims to regulate the process variables at the optimal set points. The MPC employs the finite horizon control design based on the state-space model.

This thesis consists of two main parts. In the first part, we propose a design of the integrated RTO and nominal MPC for the distillation column. The design is based on the nominal model of the distillation column. The simulation results illustrate the effectiveness of the proposed design methods. In the second part, we extend the design framework to cope with the uncertainty of the process. Thus, we propose a design of the integration of RTO and multiple MPC for the distillation column. The process dynamic is described by a set of models, where each model corresponds with a specific operating range of the distillation column. We compare the simulation results of the multiple MPC with that of the nominal MPC to determine advantages and disadvantages of each method.

ศูนย์วิทยทรัพยากร  
จุฬาลงกรณ์มหาวิทยาลัย

Department: Electrical Engineering  
Field of study: Electrical Engineering  
Academic year: 2010

Student's Signature:   
Advisor's Signature: 

## Acknowledgments

Firstly, my deepest thanks goes to my advisor, Associate Professor David Banjerdpongchai. He not only taught me useful knowledge for the research, but also help me improve some of my communication skills. I thank him for his patience, constant guidance and strong support in the academic environment and daily life. It is quite a great chance for me to work with him.

I am thankful to Associate Professor David Banjerdpongchai, Assistant Professor Manop Wongsaisuwan, Assistant Professor Suchin Arusawatwong and Associate Professor Watharapong Khovidhungij for providing me essential knowledge. It is probably a good experience for me who want to become a teaching staff member. I also acknowledge to Assistant Professor Manop Wongsaisuwan and Associate Professor Waree Kongprawechnon for willingness to be my orals and reading committee.

Many thanks to all graduate students in control systems research laboratory due to their friendliness. Interacting with Sompol, Katar, Vimonrat, Poonpak, Apichart, Anawach, Thanakorn and Somrak provides me useful education and society experience. The best wishes are given to all CRSL members. My entire study at Chulalongkorn University was financially supported by JICA Project for AUN/SEED-Net, which is gratefully acknowledged.

Finally, I would like to show my deep gratitude towards my parents for their patience and love. It is to them that I dedicate this thesis.



ศูนย์วิทยทรัพยากร  
จุฬาลงกรณ์มหาวิทยาลัย

# Contents

	Page
<b>Abstract (Thai)</b> .....	iv
<b>Abstract (English)</b> .....	v
<b>Acknowledgments</b> .....	vi
<b>Contents</b> .....	vii
<b>List of Tables</b> .....	ix
<b>List of Figures</b> .....	x
<b>CHAPTER</b> .....	xi
<b>I INTRODUCTION</b> .....	<b>1</b>
1.1 Motivation.....	1
1.2 Literature Review.....	2
1.2.1 Integration of RTO and MPC.....	2
1.2.2 Distillation Column.....	4
1.3 Research Objectives.....	6
1.4 Contributions.....	6
1.5 Thesis Outline.....	6
1.6 Conclusion.....	6
<b>II BASIC KNOWLEDGE</b> .....	<b>7</b>
2.1 Real Time Optimization.....	7
2.2 RTO for Distillation Column.....	7
2.3 Model Predictive Control.....	9
2.4 Conclusion.....	11
<b>III DYNAMIC MODEL AND CONTROL OF DISTILLATION COLUMN</b>	<b>12</b>
3.1 Dynamic Model of Distillation Column.....	12
3.2 Hankel Norm Approximation.....	15
3.3 Control of Distillation Column.....	16
3.4 Conclusion.....	16
<b>IV INTEGRATION OF RTO AND NOMINAL MPC</b> .....	<b>18</b>

CHAPTER	Page
4.1 Introduction . . . . .	18
4.2 Integration of RTO and MPC . . . . .	19
4.2.1 The 2-layer structure approach . . . . .	19
4.2.2 The 3-layer structure approach . . . . .	20
4.3 Application to Distillation Column . . . . .	22
4.3.1 Tuning Parameters . . . . .	22
4.3.2 Transient Responses . . . . .	24
4.3.3 Stability Test . . . . .	27
4.4 Conclusion . . . . .	28
<b>V INTEGRATION OF RTO AND MULTIPLE MPC . . . . .</b>	<b>30</b>
5.1 Introduction . . . . .	30
5.2 Integration of RTO and Multiple MPC . . . . .	32
5.2.1 The 2-layer structure approach . . . . .	32
5.2.2 The 3-layer structure approach . . . . .	32
5.3 Application to Distillation Column . . . . .	32
5.3.1 Tuning Parameters . . . . .	32
5.3.2 Transient Responses . . . . .	34
5.3.3 Stability Test . . . . .	38
5.4 Conclusion . . . . .	40
<b>VI CONCLUSIONS . . . . .</b>	<b>41</b>
6.1 Summary of Results . . . . .	41
6.2 Conclusion . . . . .	42
6.3 Recommendations for Future Works . . . . .	42
<b>REFERENCES . . . . .</b>	<b>43</b>
<b>APPENDIX . . . . .</b>	<b>46</b>
<b>BIOGRAPHY . . . . .</b>	<b>48</b>



## List of Tables

	Page
2.1 Parameters for the RTO problem of the Propylene splitter. . . . .	7
2.2 Optimum solutions of the RTO problem for the propylene splitter. . . . .	9
3.1 The nominal steady-state values of the Propylene splitter. . . . .	12
3.2 Product Quality Depending on the Changing of the Feed Rates. . . . .	13
4.1 Maximum allowable $C_1(\times 10^{-6}\$/\text{Btu})$ . . . . .	27
4.2 Maximum Rate of Inputs over Its Magnitude. . . . .	27
5.1 Maximum allowable $C_1(\times 10^{-6}\$/\text{Btu})$ . . . . .	38



ศูนย์วิทยทรัพยากร  
จุฬาลงกรณ์มหาวิทยาลัย

## List of Figures

	Page
1.1 Layered structure of control hierarchy. . . . .	1
1.2 The schematic diagram of a binary distillation column including the RTO layer. . . . .	5
2.1 Basic structure and MPC strategy. . . . .	10
3.1 The Location of the Distillation Column Models. . . . .	14
3.2 The output responses of the nominal models $G_0$ , $G_1$ and $G_2$ (6 states) and its corresponding linearized models (220 states). . . . .	17
3.3 The Hankel singular values of the original linearized models. . . . .	17
4.1 The state-feedback MPC controller for the distillation column based on nominal model. . . . .	18
4.2 The schematic diagram of the 2-layer structure. . . . .	19
4.3 The schematic diagram of the 3-layer structure. . . . .	20
4.4 The transient responses of system output $X_b$ and input $R$ of the 2-layer as the prediction horizon varies. . . . .	22
4.5 The transient responses of system output $X_b$ and input $R$ of the 2-layer as the control horizon varies. . . . .	23
4.6 The transient responses of system output $X_b$ and input $R$ of the 2-layer as the weighting coefficient varies. . . . .	23
4.7 The system inputs of the 2-layer, 3-layer structure. . . . .	25
4.8 The transient responses of system outputs of the 2-layer, 3-layer structure. . . . .	25
4.9 Cost functions in MPC layer and QP layer of the 2-layer and 3-layer structure. . . . .	26
4.10 Economic objective functions (after omitting the raw material cost): $C_1$ varies from $6 \times 10^{-6}$ to $9 \times 10^{-6}$ (\$/Btu) after the first 200 <sup>th</sup> min. . . . .	26
4.11 The output responses of the nominal integration approaches (2-layer and 3-layer structure) as the parameter $C_1$ (RTO layer) varies from $3 \times 10^{-6}$ \$/Btu to $10 \times 10^{-6}$ \$/Btu after the first 200 <sup>th</sup> min; ( $N_p = 10$ , $N_c = 3$ ) (case 2). . . . .	29
4.12 The input $R$ -output $X_b$ responses of the nominal integration approaches (2-layer and 3-layer structure) ( $N_p = 10$ , $N_c = 3$ ) as the limitations rate of input is 0.03 . . . . .	29
5.1 The output-feedback MPC controller for the distillation column based on the multiple models using the switching scheme. . . . .	30
5.2 The output-feedback nonadaptive MPC controller for the distillation column based on single model. . . . .	30

5.3	The integration structure of RTO and multiple MPC: (A) 2-layer approach and (B) 3-layer approach. . . . .	33
5.4	The design algorithm of the integration RTO and multiple MPC based on switch controller. . . . .	33
5.5	The transient responses of system output $X_b$ and input $R$ of the 2-layer as the prediction horizon varies. . . . .	35
5.6	The transient responses of system output $X_b$ and input $R$ of the 2-layer as the control horizon varies. . . . .	35
5.7	The transient responses of system output $X_b$ and input $R$ of the 2-layer as the weighting coefficient varies. . . . .	35
5.8	The MPC inputs of the nominal MPC and multiple MPC (2-layer structure). .	36
5.9	The MPC outputs of the nominal MPC and multiple MPC (2-layer structure). .	36
5.10	The cost of the nominal MPC and multiple MPC (2-layer structure). . . . .	36
5.11	The MPC inputs of the nominal MPC and multiple MPC (3-layer structure). .	37
5.12	The MPC outputs of the nominal MPC and multiple MPC (3-layer structure). .	37
5.13	The cost of the nominal MPC and multiple MPC (3-layer structure). . . . .	37
5.14	The output responses of the multiple integration approaches (2-layer and 3-layer structure) with ( $N_p = 10$ , $N_c=3$ ) as the parameter $C_1$ (RTO layer) varies from $3 \times 10^{-6}$ \$/Btu to $10 \times 10^{-6}$ \$/Btu after the first $200^{th}$ min (case 2). . . .	39
5.15	The output responses with the wave reference trajectory of the 2-layer structure. .	39

# CHAPTER I

## INTRODUCTION

### 1.1 Motivation

In the control hierarchy shown in Fig. 1.1, the Real Time Optimization (RTO) layer bases on measured disturbances and process outputs (the rigorous model of the plant) to optimize a given objective function at regular intervals (few hours to few days) [1]. Subsequently, the optimal solutions of the RTO layer are transferred to the Advance Process Control (APC) layer. The APC layer, usually being implemented by Model Predictive Control (MPC) strategy bases on the dynamic process model, tries to keep the controlled variables at their given set points [2].

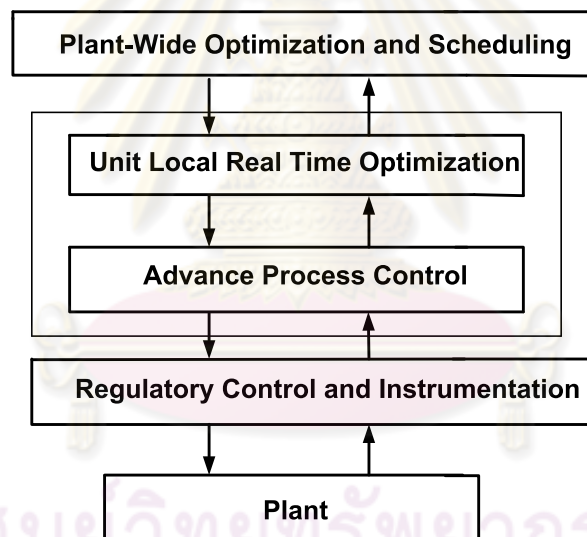


Figure 1.1: Layered structure of control hierarchy.

Increased competition in the process industry requires the improved operation with the purpose of reducing the operating cost or maximizing the profit as long as meeting the product constraints. *One of the efficient solutions* is to integrate properly the RTO layer and the MPC layer. The objectives of the integration optimization/control layers are to deal with the optimization problem as well as to guarantee the stability and the performance analysis of the system. However, there are some obstacles which cause the integration task become a challenging problem. Firstly, two layers use different kind of models: rigorous nonlinear steady state model (RTO layer) and dynamic model (MPC layer) that can cause the conflict between the reference values and the controller predictions. Secondly, two layers usually

operate at different frequencies: the sampling period of the RTO layer usually much higher than that of the control layer. Hence, the presence of disturbances or parameter uncertainties is also an important reason that changes the optimum points from the RTO layer to be the suboptimum targets for the MPC layer [1].

The theories of the integration RTO and MPC have been originated for decades. However, the formal foundations of the integration approaches are still open issues. Recent researches have been focused on the system with parametric uncertainties in the robust control framework [1, 3]. In which, the 3-layer structure with the LP/QP layer is inserted between the RTO and MPC layer is a potential direction [3–5]. There are some significant results. However, in those articles, some classes of system uncertainties have not been tackled completely and there still lacks of practical publications relating to the integration of RTO and MPC in 3-layer structure. Thus, this is still an active area.

In this research, we are interested to develop the new integration approaches of RTO and MPC in 3-layer structure based on [3, 4] by employing the simple RTO and MPC strategies. To cope with the varying of the process parameters, the multiple model predictive control (MMPC) strategy based on the state-space model is proposed in the control layer. Apart from that, developing a physical model for simulation is also a necessary requirement. In this thesis, the distillation column models which satisfy the RTO and MPC problems are constructed.

## 1.2 Literature Review

### 1.2.1 Integration of RTO and MPC

The necessity of the integration of RTO and MPC has been pointed out in section 1.1. In literature, there are several approaches being proposed to deal with the integration problem. The collection of many methods can be found in Adetola [1] and Rawlings [6].

In [7], Zanin *et al.* has presented the *1-layer approach* which includes the nonlinear economic objective function into the MPC problem. In the *1-layer approach*, the economic objective optimization is integrated within a linear MPC controller by an appropriate weighting matrix. This method responds to the change faster than the traditional 2-layer control hierarchy (Fig. 1.1). However, it is only applicable to the plants which have relatively short settings time and can be effectively described by linear models. In case of the large disturbance for the plant or the large-scale integrated plant, this method is not effective. It can lead to the high computational burden. To improve the previous work, Souza *et al.* [8] has proposed the solution by using the gradient of the economic objective function in the cost function of the controller. The main advantage of this method is that the resulting optimization/control problem can still be solved with a quadratic programming routine at each sampling step. Thus, it still preserves some of the advantages of Zanin's method and can be solved efficiently without jeopardizing the stability of the closed loop system.



The *2-layer approach* can be found in [1], [5] and [9]. In this method, the RTO problem needs not be solved at each sample time but based upon disturbance dynamics or plant condition. This method improves the computational ability of the 1-layer approach. Hence, it can be applied for large-scale systems. However, the lack of the rigorous strategy for separation of time scales and the interaction between two layers due to the different models are the disadvantages of this method since it can reduce the performance of the system. It leads to the delays in the optimization and the instability of the system. The kind of optimization techniques can be SS-RTO or D-RTO. The SS-RTO has some limitations with respect to the achievable flexibility and economic benefit; especially, as in the dynamic processes with grade transitions and batch processes [10]. Hence, the *dynamic real time optimization (D-RTO)* strategy is proposed. Instead of doing a steady state economic optimization to compute set points, a D-RTO strategy over a fixed horizon is done to compute a reference trajectory. There still exists the inconsistency between the models used in the two layers. Often, an additional disturbance model, being estimated from the output measurements, is added to resolve this inconsistency [11].

The *3-layer approach* is another method in which the LP/QP layer is inserted between the RTO layer and the MPC layer, to so called LP-MPC and QP-MPC approach. The additional layer aims to recompute the feasible targets for the inputs and outputs. This approach attempts to narrow the gap between the sampling rates of the nonlinear SS-RTO and the linear MPC. To be exact, it improves the drawback of the traditional 2-layer structure in the difference of time scales between the optimization and control layer. In Ying *et al.* [4], the set points for the MPC controller are the trajectories instead of the constant set-points as in the 2-layer approach. This article has analyzed the properties of the 3-layer approach for the *nominal system* and make a comparison with the 2-layer approach through a specific application: the Shell heavy oil fractionator. It is concluded that the 3-layer structure has some advantages in terms of robust stability and dynamic performance due to the additional layer. Recently, Alvarez *et al.* [3] has tackled with the stable integration of linear MPC and RTO in the 3-layer structure as there is *uncertainty* in the models. The proof of the system inputs-outputs converging to their targets have been done completely. This method has been developed to the case where there is the *polytopic uncertainty* in the system gains and the uncertainty in the dynamics is assumed to be of the *multi-plant* type. Generally, the 3-layer integration approach can improve the system stability and dynamic performances in comparison with the conventional 2-layer approach. However, it also leads to a complex design problem. There have a few articles relating to the stable integration in 3-layer structure. For more details, it is referred to [3–5].

The new approach, namely *Extremum Seeking Control approach*, is introduced by Guay and Adetola [1, 12, 13]. In this method, the controller drives the system states to steady state values that optimize a chosen performance objective. Krstic *et al.* [13] deals with the problem as the performance objective is directly measured online. As the performance objective is

un-measurable, Adetola *et al.* [1, 12] has proposed the solution for this problem. Generally, extremum seeking control approach can address the closed-loop stability of the overall system. However, the procedure of this method is relatively complex and the results are true only for some special classes of system.

### 1.2.2 Distillation Column

Distillation column is an industrial device which is used to implement the separating process in chemical process industries. According to Chen *et al.* [14], distillation columns account for about 40–50% total of the capital investment in a conventional fluid processing unit and 70% energy consumption of an average unit. Therefore, how to minimize the energy consumption of this device is a crucial problem in the process control because it results in relatively large improvements in overall plant operation cost. Hence, in the application parts of the thesis, the distillation column is chosen as the physical model to implement the simulation results of the integration RTO and MPC.

In terms of the RTO problem for the distillation column in literature, there are several publications. For example, Torgashov *et al.* [15] introduces sliding modes to eliminate the dependence of the process uncertainties by using a direct search strategy. Ying *et al.* [16] proposes a new strategy for the integration of RTO and MPC layer. The integration structure consists of two optimization/control levels which refer to the split ratio and radial base function. This thesis formulates the RTO problem for a distillation column as a function of the reflux ratio as the formulation of Chen *et al.* [14] with the objective of minimizing the energy consumption. Chen *et al.* [14] also shows that the following characteristics of the distillation column that are strongly favour for applications of reflux optimization:

- High reflux ratio
- High differential product values
- High utility costs
- Low relative volatility
- Feed light key far from 50%

It leads to the choice of a *propylene splitter*, the distillation column for used in the petroleum refining processes, to implement the RTO problem. The model being developed by Skogestad ([17], model D) satisfies two conditions of online optimization: **high reflux ratio** and **a relatively low volatility**. The real time optimization (RTO) problem is formulated with the purposes of minimizing the energy consumption. It is also assumed that the high utility cost fluctuates by varying one parameter in the utility cost to observe the change of the optimum values from the RTO layer. The details for the formulation and solution of the RTO problem will be shown in chapter 2. The MPC has been selected for controlling the

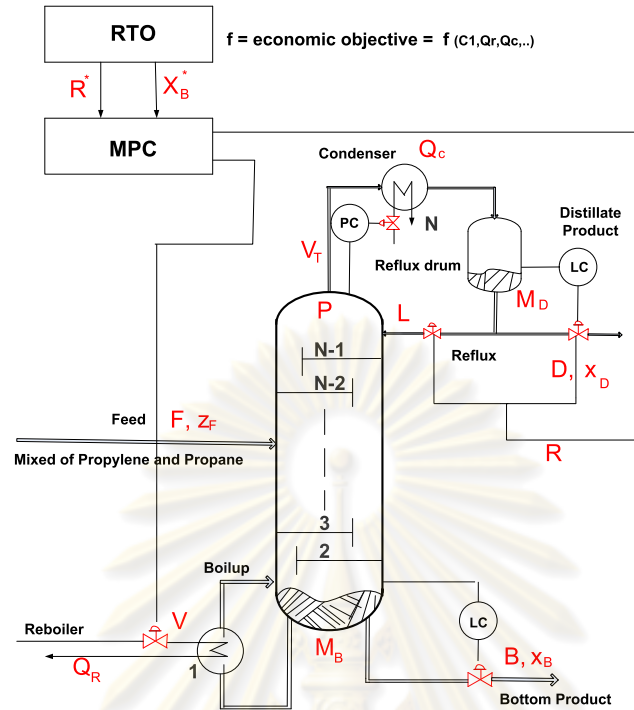


Figure 1.2: The schematic diagram of a binary distillation column including the RTO layer.

distillation column since MPC has been originally developed to meet the specialized control needs of petroleum refineries. However, distillation column is an ill-conditioned process so it is difficult to control. The conventional MPC controllers cannot provide an adequate performance with set point tracking and disturbance rejection. Several methods have been proposed to deal with this problem. For example, Minh *et al.* [18] introduces the zone control techniques to reject disturbances and maintains closed loop stability. Multivariable nonlinear MPC of an ill-conditioned distillation column can be solved by using the quasi-ARMAX model with fuzzy logic [19]. More commonly, the traditional method for controlling an ill-conditioned process with the same number of manipulated inputs as controlled outputs is to delete one or some controlled variables from the control objective. This method is used in the application section of this thesis to control the distillation column in the MPC formulation since it is simple and the probability that the MPC controller finds a solution will increase (see [18, 20] for more details). Another reason to use this method is that the distillation column has only one output target in the optimization problem. The bottom composition  $X_b$  which is controlled by the manipulated variable - the vapor flow rate  $V$ . Another output, the distillate composition  $X_d$ , is kept in an allowable range and has not appeared in the objective function since another input, the reflux ratio  $R$  is the variable from the RTO.

### 1.3 Research Objectives

The main objective of this thesis is to develop the integration of RTO and MPC in the 3-layer structure for the nominal model and multiple models. The steady-state RTO and MPC techniques are exploited to deal with the optimization problem, the stability and the performance responses of the system. Specifically, the finite horizon MPC designed bases on state-space model of the process is used in the control layer. Whereas, the steady-state RTO layer is assumed to be decoupled from the control layers (QP and MPC). In case of the variation of the parameter of the process, the multiple MPC strategy is employed.

Distillation column, a good candidate for RTO and MPC problem, is also be a part of this research. The RTO problem for the distillation column (the propylene splitter) is formulated as an RTO problem. The solution of the RTO problem gives the targets for the control layer. The dynamic model of the distillation column is developed for simulation of the controllers in the control layer. Finally, the obtained integration foundations will be compared with other integration approaches.

### 1.4 Contributions

1. A new design of the integration RTO and nominal MPC in the 3-layer structure for the distillation column.
2. A new design of the integration RTO and multiple MPC techniques in the 3-layer structure for the distillation column.

### 1.5 Thesis Outline

The organization of the thesis is as follows. Chapter 2 is the basic knowledge. Chapter 3 is about the distillation column modelling. The modified integration of RTO and MPC in the conventional 2-layer structure and 3-layer structure based on the nominal model are introduced and applied to the distillation column in chapter 4. Chapter 5 presents the integration approaches for the multiple models using multiple MPC. The conclusions and potential developments are in chapter 6.

### 1.6 Conclusion

This chapter presents the motivation and the objectives of the thesis. The literature review about the RTO problem and methods to control the distillation column is also briefly reviewed. In next chapters, the details about the integration of RTO and MPC problem are implemented.

## CHAPTER II

### BASIC KNOWLEDGE

#### 2.1 Real Time Optimization

RTO (or online optimization) is a kind of supervisory control techniques which attempts to periodically update the set points for the plant in the presence of disturbances or parameter uncertainties. The optimization strategies can be divided into steady-state real time optimization (SS-RTO) and dynamic real time optimization (D-RTO) [21].

This thesis employs the steady-state RTO strategy to implement *the integration approaches*. In SS-RTO, a *rigorous steady state model* of the process is used to calculate the set-points. The general description for the steady-state RTO problem is

$$\begin{aligned} \min_{y,u} \quad & f(y, u) \\ \text{subject to} \quad & g_1(y, u) \leq 0 \\ & g_2(y, u) = 0 \end{aligned} \quad (2.1)$$

where  $f$  represents the process economic objective based on the rigorous steady state model of the process.  $y, u$  are a set of output and input variables.  $g_1, g_2$  are sets of inequality and equality constraints which describe the behaviors of material and energy balance in the process at the steady-state [4]. The solution for this optimization problem gives the optimizing output-input targets ( $y_{\text{rto}}$  and  $u_{\text{rto}}$ ) for the Advanced Process Control layer (MPC controller).

#### 2.2 RTO for Distillation Column

Table 2.1: Parameters for the RTO problem of the Propylene splitter.

<i>Symbol</i>	<i>Description</i>	<i>Nominal Value</i>	<i>Units</i>
$C_1$	Heating cost	$3 \cdot 10^{-6}$	\$/Btu
$C_2$	Cooling cost	$9 \cdot 10^{-9}$	\$/Btu
$C_b$	Value of bottom propylene	0.26	\$/kmol
$C'_b$	Value of bottom propane	0.20	\$/kmol
$C_f$	Cost per pound of propylene	0.35	\$/kmol
$C'_f$	Cost per pound of propane	0.33	\$/kmol
$C_d$	Value of overhead propylene	0.44	\$/kmol
$C'_d$	Value of overhead propane	0.44	\$/kmol
$\lambda$	Latent heat	287	Btu/kmol

The parameters for the propylene splitter in the RTO layer are shown in table 2.1. That data comes from Chen *et.al* [14] which will be used to formulate the economic objective



function for the RTO problem of the propylene splitter. The RTO formulation is originated from the specific economic objective function of a propylene splitter [14]. Let us define

$$\begin{aligned} f &= \text{Propane sales} + \text{Propylene sales} - \text{Utility costs} - \text{Raw material costs} \quad (2.2) \\ &= \{C_d'(1 - X_d)D + C_b'(1 - X_b)B\} + \{C_d X_d D + C_b X_b B\} - \{C_1 Q_r + C_2 Q_c\} \\ &\quad - \{C_f X_f F + C_f'(1 - X_f)F\} \end{aligned}$$

where the steady-state values are in table 3.1 [17] and all parameters for RTO problem are in table 2.1 [14]. It is noted that the Raw material costs (two final elements of Eq. 2.2 with  $C_f$ ,  $C_f'$ ,  $F$  and  $X_f$ ) are assumed to be constant during the process. It is also assumed that  $Q_r = Q_c = \lambda V$  ( $\lambda$  is the average latent heat per unit of mass,  $V$  is the vapor boil-up in mass).

In accordance with the economic objective function in the Eq. 2.2, other equations being used to describe the steady-state behaviors in the distillation column (the *rigorous nonlinear steady-state model* as [14], [22]) include.

The minimal reflux ratio at which the desired top composition can be obtained

$$R_m = \frac{1}{\alpha - 1} \left( \frac{X_d}{X_f} - \frac{1 - X_d}{1 - X_f} \right) \quad (2.3)$$

The Eduljee correlation: to find the minimal trays  $N_m$

$$\frac{N - N_m}{N + 1} = \frac{3}{4} \left( 1 - \left( \frac{R - R_m}{R + 1} \right)^{0.5668} \right) \quad (2.4)$$

The Fenske equation: to compute the bottom composition  $X_b$

$$N_m = \frac{\ln \left( \frac{X_d}{1 - X_d} \cdot \frac{1 - X_b}{X_b} \right)}{\ln(\alpha)} \quad (2.5)$$

The overall material balance and the component material balance are used to derive the bottom and overhead flow rate.

$$F = D + B \quad (2.6)$$

$$X_f F = X_d D + X_b B \quad (2.7)$$

The optimization variables are defined based on two variables: the reflux ratio  $R$  and the bottom product purity  $X_b$ .

• **The Procedure to Solve the Optimization Problem (2.2-2.6) as follows.**

1. All variables are transformed into the manipulated variable - the reflux ratio  $R$ .

2. The distillate composition  $X_d$  is assumed to be fixed at its minimum value (0.99 mole fraction) as in Edgar [23].
3. Other variables are derived from the variable  $R$ . The range of variables in  $g_1$  are defined specifically in the chapter 3.  $g_2$  is derived from (2.3 - 2.6).
4. As a results, the steady-state RTO problem for the distillation column can be quantified as the optimization problem

$$\begin{aligned} & \max_R f(R) & (2.8) \\ \text{subject to } & g_1(R) \leq 0 \\ & g_2(R) = 0 \end{aligned}$$

where

$$g_1(R) = \begin{bmatrix} R - R_{\max} \\ R_{\min} - R \\ X_b - X_{b\max} \\ X_{b\min} - X_b \\ V - V_{\max} \\ V_{\min} - V \end{bmatrix}$$

5. The *Optimization Toolbox of MATLAB* with the command *fmincon* is used to solve the optimization problem (2.8) which gives the optimizing input target for the control layer  $R_{\text{rto}}$ . Then, the optimizing output target  $X_{\text{brto}}$  is derived from (2.6).

The solutions for the RTO problem as the parameter  $C_1$  in the *utility cost* varies from  $3 \times 10^{-6}$  to  $17 \times 10^{-6}$  (\$/Btu) are shown in the Table 2.2. That optimizing targets will be the setpoints for the MPC controllers.

Table 2.2: Optimum solutions of the RTO problem for the propylene splitter.

$C_1 (\times 10^{-6})$	$R_{\text{rto}}$	$X_{\text{brto}}$	$C_1 (\times 10^{-6})$	$R_{\text{rto}}$	$X_{\text{brto}}$	$C_1 (\times 10^{-6})$	$R_{\text{rto}}$	$X_{\text{brto}}$
3	19.02	0.032	8	16.86	0.067	13	15.92	0.099
4	18.35	0.040	9	16.64	0.073	14	15.79	0.106
5	17.86	0.046	10	16.43	0.079	15	15.65	0.113
6	17.46	0.053	11	16.23	0.086	16	15.52	0.120
7	17.14	0.060	12	16.00	0.096	17	15.46	0.124

### 2.3 Model Predictive Control

The term Model Predictive Control (MPC) does not designate a specific control strategy but a very ample range of control methods which make an explicit use of a model of the process to obtain the control signal by minimizing an objective function. Normally, the standard MPC process composes of three steps: future state/output prediction, objective function optimization and control signal implementation. In which, the model is the corner stone which is used to explicitly generate the future state/output prediction based on the control

implementation and the values up to the instant time  $t$ . Whereas, the optimizer block is used to generate the control signal implementation based upon the specific objective function optimization and the predefined constraints (Fig. 2.1). Generally, the main advantages of MPC are summarized as follows [21]:

- Efficient handling of a large number of variables and handling constraints.
- The optimization problem can be formulated in a number of ways.
- Efficient control where the variables are highly interactive.
- Feed forward capabilities for measured disturbances.

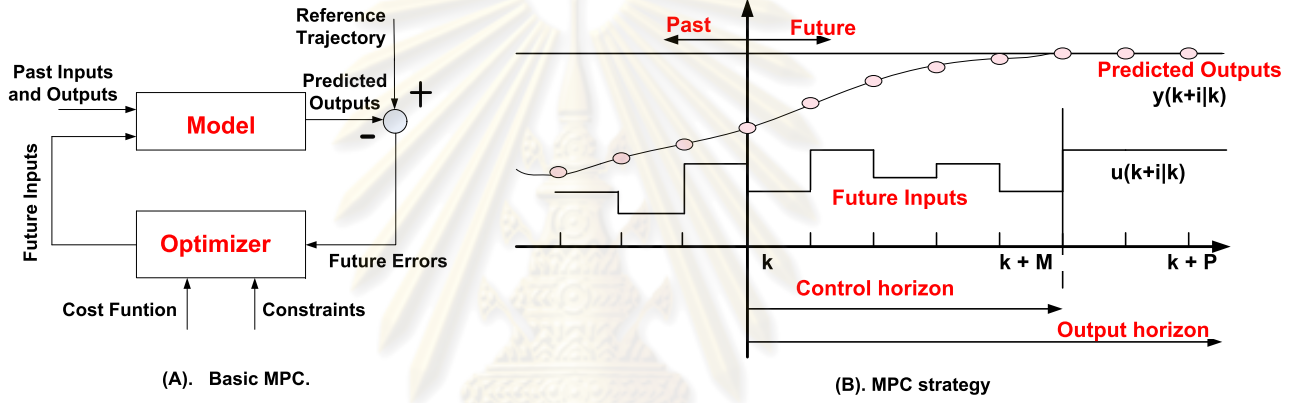


Figure 2.1: Basic structure and MPC strategy.

In this thesis, the finite horizon MPC strategy is used to implement the integration approaches in accordance with the steady-state RTO in section 2.1. Finite horizon model predictive control (MPC) is the MPC strategy in which the length of the prediction horizon and control horizon are finite. The *state-space model* for the discrete-time system is assumed as [24]

$$x_m(k+1) = A_m x_m(k) + B_m u(k) \quad (2.9)$$

$$y(k) = C_m x_m(k)$$

where  $x_m(k) \in \mathbb{R}^{n_x}$ ,  $y(k) \in \mathbb{R}^{n_y}$  and  $u(k) \in \mathbb{R}^{n_u}$  are state, output and input, respectively. Let  $\Delta x_m(k) = x_m(k+1) - x_m(k)$ ,  $\Delta u(k) = u(k+1) - u(k)$ , the state-space model with incremental form to implement the MPC problem is derived as

$$x(k+1) = Ax(k) + B\Delta u(k) \quad (2.10)$$

$$y(k) = Cx(k)$$

where

$$x(k) = \begin{bmatrix} \Delta x_m(k) \\ y(k) \end{bmatrix}, \quad A = \begin{bmatrix} A_m & 0_m \\ C_m A_m & I_m \end{bmatrix}, \quad B = \begin{bmatrix} B_m \\ C_m B_m \end{bmatrix}, \quad C = [0_m \quad I_m].$$

Note that  $x(k) \in \mathbb{R}^n$  where  $n = n_{x_m} + n_y$  and let  $D_0 = C_m B_m$  be the static gain of the system. According to Boom *et. al.* [25], the state-space model with incremental form will give a good steady-state behavior in the presence of the reference signal. For the MPC reference tracking problem including output-input targets, let us define the objective function as

$$J = \sum_{j=k+1}^{k+N_p} \|y(j|k) - y_{\text{set}} - \theta_k\|_Q^2 + \sum_{j=k+1}^{k+N_c} \|u(j|k) - u_{\text{set}}\|_E^2 \quad (2.11)$$

$$+ \sum_{j=k+1}^{k+N_c} \|\Delta u(j|k)\|_S^2 + \theta_k^T P \theta_k$$

where

- $Q$ ,  $E$ ,  $S$  and  $P$  are positive definite weighting matrices;
- $N_p$  and  $N_c$  are the prediction horizon and control horizon;
- $y_{\text{set}}$  and  $u_{\text{set}}$  are optimizing output and input targets;
- $\theta_k$  is the slack variable that is inserted to enlarge the feasible domain of the MPC problem.

The formulation of the optimization problem (2.11) includes both input-output targets. Typically, in the RTO layer, the real time optimizer is used to compute the economic target values for both output and some input variables. As being stated in Brosilow [26], the formulation (2.11) is in case of the number of inputs exceeds the number of controlled variables ( $n_u \geq n_y$ ). In that case, it is desirable (from an economic point of view) to also try to achieve some setpoints on the manipulated input variables from the RTO layer by adding a cost term

$$\sum_{j=k+1}^{k+N_c} \|u(j|k) - u_{\text{set}}\|_E^2.$$

The general MPC formulation becomes

$$\min_{\theta_k, \Delta \mathbf{u}_k} J$$

subject to

$$\left. \begin{aligned} y_{\min} &\leq y(j|k) \leq y_{\max}, & j &= k+1, \dots, k+N_p \\ u_{\min} &\leq u(j|k) \leq u_{\max}, & j &= k+1, \dots, k+N_c \\ |\Delta u(j|k)| &\leq \Delta u_{\max}, & j &= k+1, \dots, k+N_c \end{aligned} \right\} \quad (2.12)$$

where  $\Delta \mathbf{u}_k = [\Delta u(k+1|k)^T \ \Delta u(k+2|k)^T \ \dots \ \Delta u(k+N_c|k)^T]^T$ . The first element of the implementation control input at the  $k^{\text{th}}$  sample which will be transferred into the process.

## 2.4 Conclusion

This chapter presents briefly about the basic knowledge of real time optimization and model predictive control. The RTO for distillation column based on the rigorous model is formulated and solved. The finite horizon MPC strategy which is used for the integration approaches in this thesis is also presented. The RTO solution of the distillation column will be used in the next chapters for the simulation.

## CHAPTER III

# DYNAMIC MODEL AND CONTROL OF DISTILLATION COLUMN

### 3.1 Dynamic Model of Distillation Column

As being stated in chapter 1, the propylene-propane splitter (model D-Skogestad [17]) is used in this thesis. The RTO problem for this distillation column is formulated and solved in chapter 2 based on the rigorous model and data from [14]. The solution of the RTO problem gives the optimum reflux ratio  $R$  and the bottom composition  $X_b$ . To incorporate with the MPC controller appropriately, the distillation column model with the  $R - V$  structure is chosen. The first input of the dynamic model, reflux ratio  $R$ , is the variable that is driven to track the target from the RTO layer. The second input, vapor flowrate  $V$ , is responsible for driving the output  $X_b$  track the target from the RTO layer.

Table 3.1: The nominal steady-state values of the Propylene splitter.

<i>Symbol</i>	<i>Description</i>	<i>Nominal Value</i>	<i>Units</i>
$B$	Bottom flow rate	0.39	kmol/min
$D$	Overhead flow rate	0.61	kmol/min
$L$	Liquid flow rate	11.86	kmol/min
$V$	Vapor flow rate	12.48	kmol/min
$F$	Feed rate (mixed of Propylene-Propane)	1.00	kmol/min
$R^{(*)}$	Reflux ratio ( $= L/D$ )	19.32	
$X_b^{(*)}$	Fraction of propylene in the bottom product	0.10	mole fraction
$X_d$	Fraction of propylene in the top product	0.995	mole fraction
$X_f$	Fraction of propylene in the feed flow	0.65	mole fraction
$q_f$	Nominal fraction of liquid in feed	1	
$N = N_T$	Number of trays	110	
$\tau$	Time constant for liquid dynamics	0.014	min
$N_f$	Feed at stage	39	
$M_i$	Liquid holdup on each stage	0.50	kmol
$\alpha$	Relative volatility	1.12	
$(*)$	<i>Variables with optimum targets from the RTO layer</i>		

In this chapter, with the attempt of constructing the dynamic models for the Advance Process Control layer (MPC controllers), the Skogestad's package [27] is used. The package includes of 5 files: `colamod.m`, `colarv.m`, `cola_linearized.m`, `cola_rvlin.m`, `command_colarv.m`.



The function of each file is as follows.

- File `colamod.m` contains all the basic column model equations.
- File `colarv.m` MATLAB interface to `colamod.m` with the close level loops (distillate and bottom flowrate  $D$ ,  $B$  are used to control reboiler and condenser holdup  $M_D$ ,  $M_B$ ).
- File `cola_linearized.m` and `cola_rvlin.m` are used to create the linearized model around some specific equilibrium point for the distillation column. The linearized models are in the state-space form which contains  $2N_T$  number of states ( $N_T$ : number of trays of the distillation column).
- File `command_colarv.m` contains all the commands to create the linearized models and truncate the linearized model. The linearized system ( $2N_T$  states) are truncated by using the balance realization and Hankel approximation criterion upto small number of states (see [27], [28] for more details).

The nonlinear equations that describes the distillation column operation are shown in Appendix chapter. The investigation of the varying of product quality according to the change of the feed rate for the propylene splitter gives the results in the table 3.2. The objectives of the control problem for the distillation column is to keep the quality product in the ranges ( $X_b \leq 20\%$ ,  $X_d \geq 99\%$ ). As can be seen, at the nominal operating condition of the feedrate, the distillate composition and the bottom composition are in the allowable range. However, as the feedrate is reduced by 10%, the distillate composition is strictly reduced. As the feedrate is increased by 10%, the bottom composition is increased over the maximum allowable value. In the remaining of the thesis, we assume that the feedrate does not change during the operation of the process.

Table 3.2: Product Quality Depending on the Changing of the Feed Rates.

Case	Distillate Composition $X_D$ %	Bottom Composition $X_B$ %
Normal Feed rate	99.48	10.17
Reduced Feed rate by 10%	94.33	2.06
Increased Feed rate by 10%	99.65	21.42

In order to obtain the linear model from a nonlinear model, it is assumed that the variables deviate only slightly from some operating conditions, then the nonlinear equation can be expanded into a Taylor's series. In this thesis, two files (`cola_linearized.m`, `cola_rvlin.m`) will be used to implement the linearization. The linearization of the control model leads to  $220^{th}$  order linear model in the state space form around the steady-state value.

$$\begin{aligned} \dot{z}(t) &= Az(t) + Bu(t) \\ y(t) &= Cz(t) \end{aligned} \quad (3.1)$$

where

$$z(t) = \begin{bmatrix} x_1(t) - \bar{x}_{1,ss} \\ x_2(t) - \bar{x}_{2,ss} \\ \vdots \\ x_{220}(t) - \bar{x}_{220,ss} \end{bmatrix}, \quad y(t) = \begin{bmatrix} x_1(t) - \bar{x}_{1,ss} \\ x_{220}(t) - \bar{x}_{220,ss} \end{bmatrix}, \quad u(t) = \begin{bmatrix} R(t) - \bar{R}_{ss} \\ V(t) - \bar{V}_{ss} \end{bmatrix}$$

The steady-state gain is

$$D_{(0)} = -CA^{-1}B$$

The full-order linear model which represents a two inputs-two outputs in Eq. 3.1 is then reduced to low order linear model using Hankel norm approximation. The small order linear model (6 states) is suitable to become the prediction model of the MPC controllers. In this thesis, we use this method to determine 3 linearized models corresponding with 3 values of the reflux ratio  $R$  (according to the solution of the RTO problem - table 2.2).

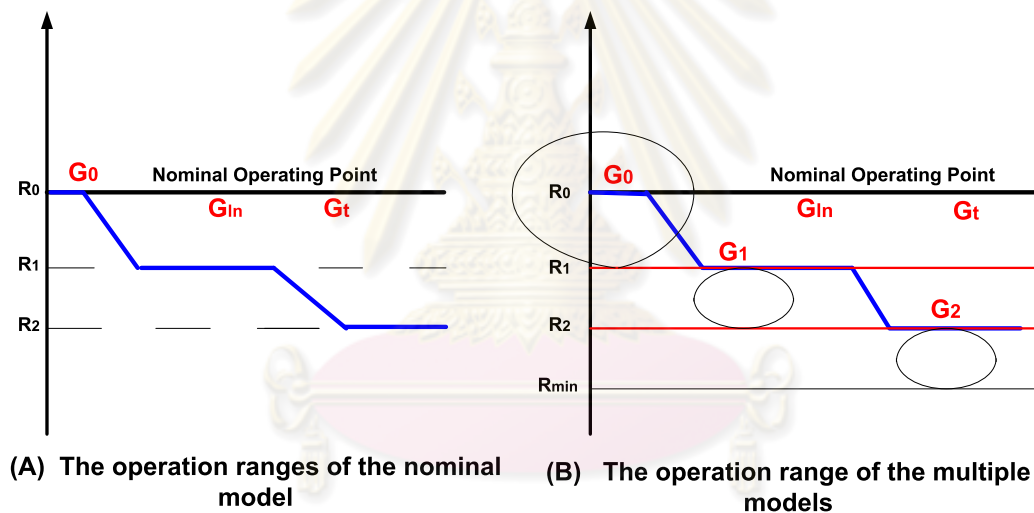


Figure 3.1: The Location of the Distillation Column Models.

The simplified state space models with 6 states are as follows.

- Nominal operating point (model  $G_0$ ):  $R_0 = 19.32$ ;  $V_0 = 12.476$  (kmol/min);  $X_{d0} = 0.995$  (mole fraction);  $X_{b0} = 0.106$  (mole fraction);  $F_0 = 1.00$ ;  $Z_{F0} = 0.65$ .

$$A = \begin{bmatrix} -0.621 & -4.827 & 0.848 & 0.142 & 0.059 & -0.548 \\ 5.440 & -0.672 & -1.305 & 1.712 & -0.016 & -0.203 \\ 0 & 0 & -0.956 & -1.230 & -0.010 & 0.111 \\ 0 & 0 & 2.338 & -1.396 & 0.052 & 0.332 \\ 0 & 0 & 0 & 0 & -0.007 & 0.001 \\ 0 & 0 & 0 & 0 & 0 & -0.047 \end{bmatrix}, \quad B = \begin{bmatrix} 0.001 & 0.033 \\ -0.001 & -0.079 \\ -0.005 & -0.195 \\ -0.0002 & 0.057 \\ -0.012 & 0.021 \\ -0.009 & 0.013 \end{bmatrix},$$

$$C = \begin{bmatrix} 0 & 0 & 0 & 0 & -0.002 & 0.001 \\ -0.089 & -0.012 & 0.075 & 0.163 & -0.026 & -0.035 \end{bmatrix}.$$

The eigenvalues of  $A$  are  $(-0.647 \pm 5.124 i; -1.176 \pm 1.681i; -0.007; -0.047)$ , hence the linear system at  $G_0$  is stable.

- Model  $G_1$ :  $R = 17.462$ ;  $V = 11.336$  (kmol/min);  $X_d = 0.992$  (mole fraction);  $X_b = 0.107$  (mole fraction) (corresponding with  $C_1 = 6 \times 10^{-6}$  \$/Btu - table 2.2).

$$A_1 = \begin{bmatrix} -0.572 & 4.854 & -0.308 & 0.738 & -0.216 & 0.065 \\ -5.391 & -0.722 & -2.107 & -0.441 & 0.088 & 0.007 \\ 0 & 0 & -1.668 & 1.444 & 0.107 & 0.019 \\ 0 & 0 & -2.109 & -0.690 & 0.242 & -0.009 \\ 0 & 0 & 0 & 0 & -0.0210 & \\ 0 & 0 & 0 & 0 & 0 & -0.006 \end{bmatrix}, B_1 = \begin{bmatrix} 0.001 & 0.024 \\ 0.001 & 0.082 \\ 0.004 & 0.190 \\ -0.003 & -0.080 \\ -0.010 & 0.019 \\ -0.015 & 0.018 \end{bmatrix},$$

$$C_1 = \begin{bmatrix} 0 & 0 & 0 & 0 & 0.001 & -0.003 \\ -0.091 & 0.002 & 0.045 & 0.177 & -0.036 & -0.021 \end{bmatrix}.$$

The eigenvalues of  $A_1$  are  $(-0.647 \pm 5.115i; -1.179 \pm 1.675i; -0.021; -0.0061)$ , hence the linear system at  $G_1$  is stable.

- Model  $G_2$ :  $R = 16.643$ ;  $V = 10.833$  (kmol/min);  $X_d = 0.989$  (mole fraction);  $X_b = 0.110$  (mole fraction) (corresponding with  $C_1 = 9 \times 10^{-6}$  \$/Btu - table 2.2).

$$A_2 = \begin{bmatrix} -0.466 & 5.246 & -0.490 & 1.707 & -0.135 & 0.030 \\ -4.931 & -0.822 & 1.173 & -0.609 & -0.087 & 0.054 \\ 0 & 0 & -0.783 & -1.340 & 0.102 & -0.024 \\ 0 & 0 & 2.181 & -1.564 & 0.228 & -0.004 \\ 0 & 0 & 0 & 0 & -0.020 & 0 \\ 0 & 0 & 0 & 0 & 0 & -0.006 \end{bmatrix}, B_2 = \begin{bmatrix} 0.007 & -0.058 \\ 0.002 & 0.062 \\ -0.005 & -0.187 \\ -0.005 & 0.091 \\ -0.011 & 0.021 \\ -0.015 & 0.017 \end{bmatrix},$$

$$C_2 = \begin{bmatrix} 0 & 0 & 0 & 0 & 0.002 & -0.004 \\ -0.044 & -0.081 & 0.107 & 0.151 & -0.037 & -0.019 \end{bmatrix}.$$

The eigenvalues of  $A_2$  are  $(-0.644 \pm 5.083 i; -1.173 \pm 1.664i; -0.020; -0.006)$ , hence the linear system at  $G_2$  is stable.

The responses of each model corresponding with the step in each input channel are shown in Fig. 3.2. The Fig. 3.2 shows that the responses of the model  $G_1$  and the model  $G_2$  are close to each other. Whereas, in comparison with different nominal linear model, the model  $G_0$  seems to give the most displacements with the responses of  $G_1$  and  $G_2$ . The Hankel singular values of the original linearized models are shown in Fig. 3.3. Since the truncated models have 6 states, the 7<sup>th</sup> singular value on the Fig. 3.3 demonstrates the result of the approximation approach for each full linearized model.

### 3.2 Hankel Norm Approximation

- The Hankel norm of a stable system is obtained when one applies an input  $w(t)$  up to  $t = 0$  and measures the output  $z(t)$  for  $t > 0$ , and select  $w(t)$  to maximize the ratio of the 2-norms

of these two signals.

$$\|G(s)\|_H := \max_{w(t)} \frac{\sqrt{\int_0^\infty \|z(t)\|_2^2 dt}}{\sqrt{\int_{-\infty}^0 \|w(t)\|_2^2 dt}} \quad (3.2)$$

The Hankel norm is a kind of induced norm from past inputs to future outputs. It can be shown that the Hankel norm in Eq. 3.2 is equivalent to the value:

$$\|G(s)\|_H := \sqrt{\rho(PQ)} \quad (3.3)$$

where  $P$ ,  $Q$  are the controllability Gramian and observability Gramian [28]. The corresponding Hankel singular values are the positive square roots of the eigenvalues of  $PQ$ .

$$\sigma_i := \sqrt{\lambda_i(PQ)} \quad (3.4)$$

- Optimal Hankel norm approximation: given a stable model  $G(s)$  of order  $n$ , find a reduced order  $G_h^k(s)$  of degree  $k$  such that the Hankel norm of the approximation error  $\|G(s) - G_h^k(s)\|_H$  is minimized. According to Skogestad [28], the Hankel norm of error between  $G(s)$  and the truncated model  $G_h^k(s)$  is equal to the  $(k + 1)^{th}$  Hankel singular value of  $G(s)$ .

### 3.3 Control of Distillation Column

Apart from tracking to the targets from RTO layer, it is also required to drive the outputs of the distillation column ( $X_d$ ,  $X_b$ ) in the allowable range to guarantee the quality of the product. The inputs are also be restricted in the specific ranges due to the limitation of the controller. We uses the term deviation for the input of this distillation column model.

1. Inputs ( $R$ ,  $V$ ) are allowed to vary within  $\pm 100\%$  of their nominal values:  
 $0 \leq V \leq 25.728$  (kmol/min) and  $0 \leq R = L/D \leq 38.642$ .
2. Disturbances  $F$ ,  $Z_F$  are assumed to be constant.
3. The output constraints are  $0.99 \leq X_d \leq 1.00$  (mole fraction) and  $0 \leq X_b \leq 0.20$  (mole fraction).
4. The rate of input constraints are  $0 \leq |\Delta R/\Delta t| \leq 19.32$  and  $0 \leq |\Delta V/\Delta t| \leq 12.864$  (kmol/min<sup>2</sup>).

### 3.4 Conclusion

This chapter introduces the operation of a distillation column. The appropriate dynamic models of this distillation column are derived. Subsequently, the MPC controller configuration which are used for the nominal and multiple models based design are shown. The results of this chapter will be used for the applications of the theoretical foundation in next chapters.

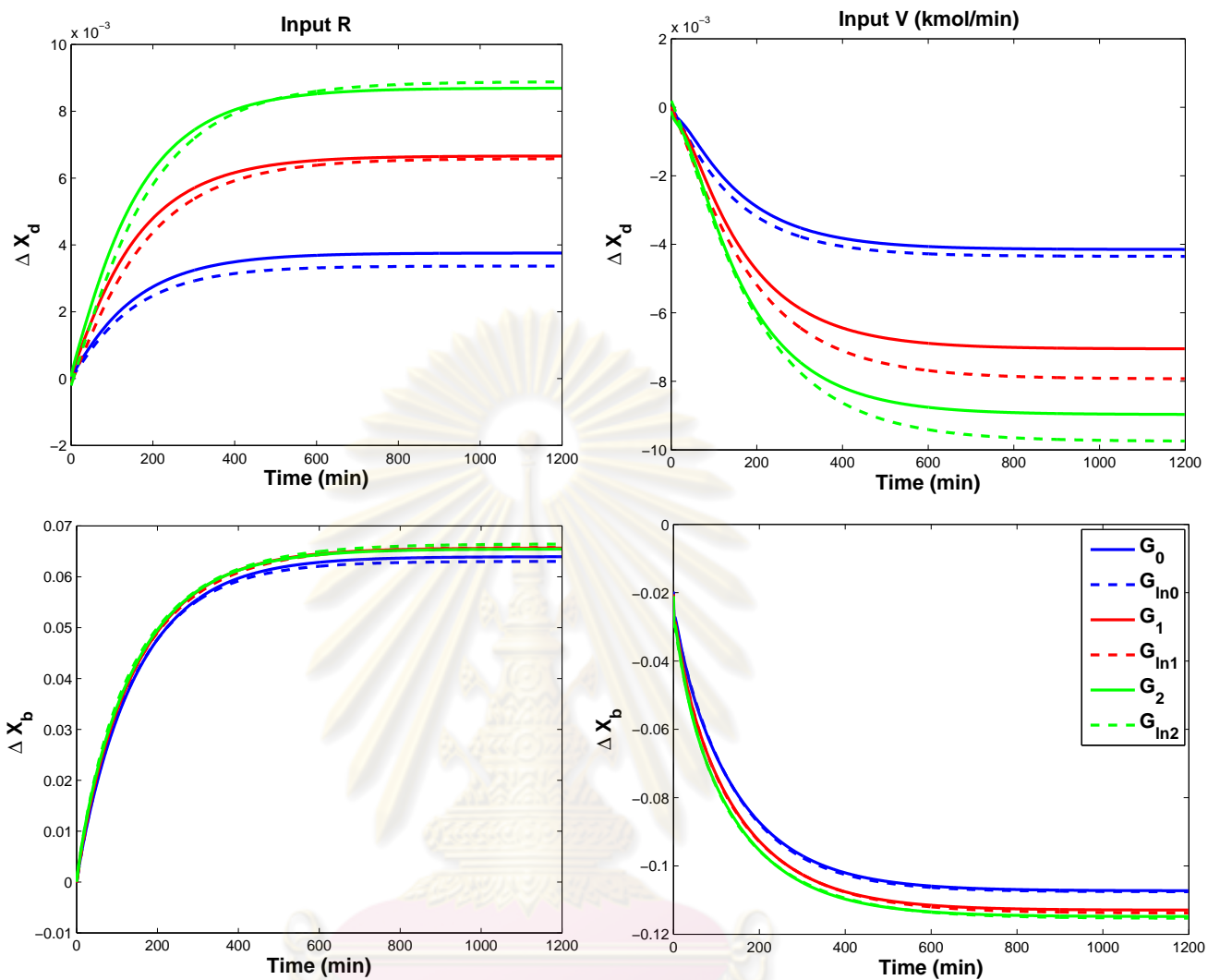


Figure 3.2: The output responses of the nominal models  $G_0$ ,  $G_1$  and  $G_2$  (6 states) and its corresponding linearized models (220 states).

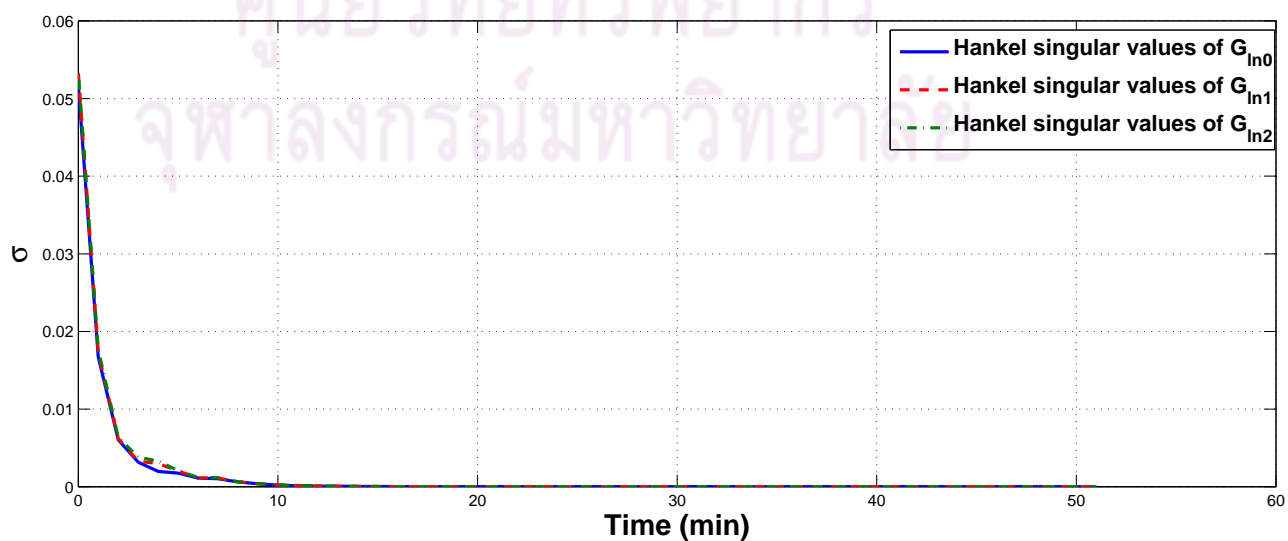


Figure 3.3: The Hankel singular values of the original linearized models.



## CHAPTER IV

### INTEGRATION OF RTO AND NOMINAL MPC

#### 4.1 Introduction

In this chapter, the integration of RTO and MPC in the 2-layer and the 3-layer structures based on the nominal state-space model are derived. The steady-state RTO and the finite horizon MPC are used to do the integration approaches. In the MPC problem of the nominal case (chapter 4), we assume that there is only nominal model ( $G_0$  - chapter 3) being used for the MPC controller and it also demonstrates the actual process model. Hence, the mismatch between the model and the actual process is not taken into account in this chapter. In this case, the state feedback controller is used in the design. The MPC controller based design is as follows.

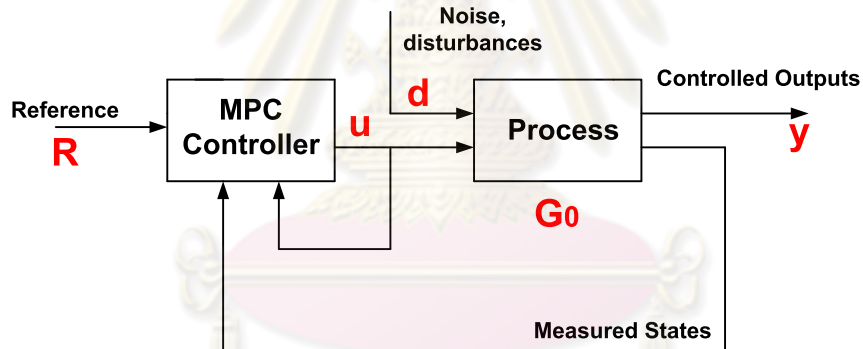


Figure 4.1: The state-feedback MPC controller for the distillation column based on nominal model.

In the proposed integration methods (this chapter and chapter 5), we assume that the RTO layer is dynamically decoupled from the control layers with the sampling period  $T_{rto}$  in the unit of hours. The sampling period of the control layers (QP/MPC) are the same units of minutes. The controllers receive the optimizing targets from the RTO layer. There are no interactions from the control layers toward the RTO layer. Note that the *steady-state rigorous model* is used for the RTO layer and the *dynamic linear model* as distillation column model (chapter 3) is used for control layer.

## 4.2 Integration of RTO and MPC

### 4.2.1 The 2-layer structure approach

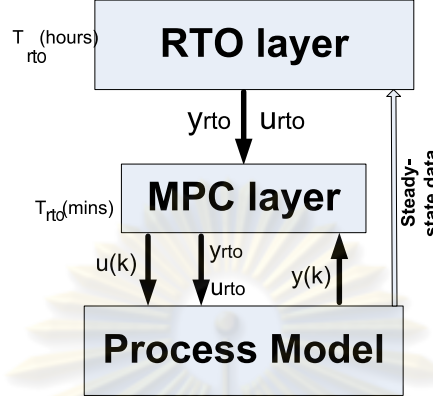


Figure 4.2: The schematic diagram of the 2-layer structure.

Enforcing a strict constraint that  $y = y_{\text{set}}$  and  $u = u_{\text{set}}$  at all times will lead to infeasible MPC problem. Hence, to integrate the RTO layer with the MPC layer in this work, the MPC controller is defined with two additional constraints for the terminal output-input targets to equal their desired values at the end of prediction and control horizon. To enlarge the feasible region, the soft constraints are used in the output targets by defining the slack variable  $\theta_{y,k}$ .

*The MPC problem*

$$\min_{\theta_{y,k}, \Delta \mathbf{u}_k} J_1 \quad (4.1)$$

subject to (2.12) and

$$y(k|k + N_p) - y_{\text{rto}} - \theta_{y,k} = 0 \quad (4.1a)$$

$$u(k-1) - u_{\text{rto}} + I_u^T \Delta \mathbf{u}_k = 0 \quad (4.1b)$$

where  $J_1$  is defined as in (2.11) with modifications:  $y_{\text{set}}$ ,  $u_{\text{set}}$  and  $\theta_k$  are replaced by  $y_{\text{rto}}$ ,  $u_{\text{rto}}$  and  $\theta_{y,k}$ , respectively. Constraints (4.1a, 4.1b) are for the terminal outputs-inputs, respectively. To solve the MPC problem, the cost function  $J_1$  is rewritten as

$$J_1 = \begin{bmatrix} \Delta \mathbf{u}_k \\ \theta_{y,k} \end{bmatrix}^T H \begin{bmatrix} \Delta \mathbf{u}_k \\ \theta_{y,k} \end{bmatrix} + C_f^T \begin{bmatrix} \Delta \mathbf{u}_k \\ \theta_{y,k} \end{bmatrix} + C_e \quad (4.2)$$

where

$$H = \begin{bmatrix} \Phi^T Q_1 \Phi + S_1 + M^T E_1 M & -\Phi^T Q_1 I_y \\ -I_y^T Q_1 \Phi & I_y^T Q_1 I_y + P \end{bmatrix}$$

$$C_f = \begin{bmatrix} 2\Phi^T Q_1 \left( \Pi x(k)^T - I_y y_{\text{rto}} \right) + 2M^T E_1 I_u^T (u(k-1) - u_{\text{rto}}) \\ -2I_y^T Q_1 \left( \Pi x(k)^T - I_y y_{\text{rto}} \right) \end{bmatrix}$$

$$C_e = (u(k-1) - u_{rto})^T I_u E_1 I_u^T (u(k-1) - u_{rto}) + \left( x(k)^T \Pi^T - y_{rto}^T I_y^T \right) Q_1 (\Pi x(k) - I_y y_{rto})$$

and

$$Q_1 = \begin{bmatrix} Q & & 0 \\ & \ddots & \\ 0 & & Q \end{bmatrix}, \quad E_1 = \begin{bmatrix} E & & 0 \\ & \ddots & \\ 0 & & E \end{bmatrix}, \quad S_1 = \begin{bmatrix} S & & 0 \\ & \ddots & \\ 0 & & S \end{bmatrix}$$

$$M = \begin{bmatrix} I_{nu} & 0 & \cdots & 0 \\ I_{nu} & I_{nu} & \cdots & 0 \\ \vdots & \vdots & \ddots & \vdots \\ I_{nu} & I_{nu} & \cdots & I_{nu} \end{bmatrix}, \quad \Pi = \begin{bmatrix} CA \\ CA^2 \\ \vdots \\ CA^{N_p} \end{bmatrix}, \quad \Phi = \begin{bmatrix} CB & 0 & 0 & \cdots & 0 \\ CAB & CB & 0 & \cdots & 0 \\ \vdots & \vdots & \vdots & \ddots & \vdots \\ CA^{N_p} B & CA^{N_p-1} B & \cdots & \cdots & CA^{N_p-N_c} B \end{bmatrix}$$

$$I_y = [I_{ny} \ I_{ny} \ \cdots \ I_{ny}]^T \in \mathbb{R}^{(n_y \cdot n_{xm}) \times (n_y)}, \quad I_u = [I_{nu} \ I_{nu} \ \cdots \ I_{nu}]^T \in \mathbb{R}^{(n_u \cdot n_{xm}) \times (n_u)}.$$

The MPC problem becomes to minimize the quadratic function (4.2), subject to constraints of the problem (4.1).

This approach is based on the conventional optimization-control structure (2-layer structure). As being stated in section 2.3, the disadvantage of the formulation (4.1) is that unless there is sufficient degree of freedom to drive the objective function  $J$  to zero, we will have the steady-state in which all of the input and output values do not reach the setpoint.

#### 4.2.2 The 3-layer structure approach

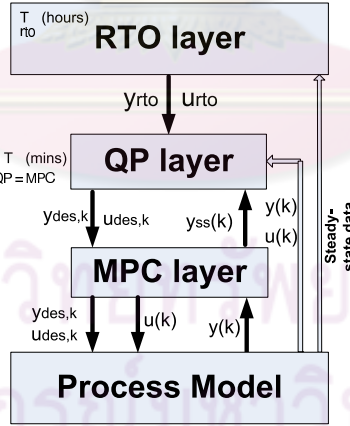


Figure 4.3: The schematic diagram of the 3-layer structure.

In this section, the 3-layer integration structure is introduced. It differs to the 2-layer structure in which the QP layer is inserted to re-compute the achievable set points for the MPC layer (Figure 4.3). By regularly updating the setpoints for the MPC layer at each sampling instant of the MPC controller using the QP layer, it probably increases the feasible domain for the optimizer in case of the disturbance or parameter varying in the RTO layer [4]. The simulation results in next section will show more details about the difference of this integration structure with the 2-layer structure.

Let us define

$$J_2 = \|y_{\text{des}} - y_{\text{rto}}\|_{Q_y} + \|u_{\text{des}} - u_{\text{rto}}\|_{Q_u} + \|\epsilon_k\|_{Q_\epsilon}$$

The QP problem becomes

$$\min_{y_{\text{des},k}, u_{\text{des},k}, \epsilon_k} J_2 \quad (4.3)$$

subject to

$$\begin{aligned} u_{\min} &\leq u_{\text{des},k} \leq u_{\max} \\ y_{\min} + \epsilon_k &\leq y_{\text{des},k} \leq y_{\max} + \epsilon_k \\ y_{\text{des},k} - y_{\text{ss},k-1} &= [u_{\text{des},k} - u(k-1)] D_0 \\ -N_c \Delta u_{\max} &\leq u_{\text{des},k} - u(k-1) \leq N_c \Delta u_{\max} \end{aligned}$$

where  $Q_y$ ,  $Q_u$  and  $Q_\epsilon$  are positive definite weighting matrices;  $\epsilon_k$  is a slack variable that softens the bound  $y_{\text{des},k}$ . The formulation is based on Alvarez [3].  $D_0$  is the static gain of the system. In this case, the predicted steady-state output  $y_{\text{ss},k-1} = y(k + N_p - 1 | k - 1)$ .

The MPC problem is defined as

$$\min_{\theta_{y,k}, \Delta \mathbf{u}_k} J_3 \quad (4.4)$$

subject to (2.12) and

$$y(k | k + N_p) - y_{\text{des},k} - \theta_{y,k} = 0 \quad (4.4a)$$

$$u(k-1) - u_{\text{des},k} + I_u^T \Delta \mathbf{u}_k = 0 \quad (4.4b)$$

where  $J_3$  is defined as in Eq. 2.11 with modifications:  $y_{\text{set}}$ ,  $u_{\text{set}}$  and  $\theta_k$  are replaced by  $y_{\text{des},k}$ ,  $u_{\text{des},k}$  and  $\theta_{y,k}$ , respectively. Constraints (4.4a), (4.4b) are the terminal output, input targets.

**Remark 1:**

All the MPC problems and QP problem have been transferred into a general QP problem:

$$\begin{aligned} \min_{\mathbf{x}} \quad & \frac{1}{2} \mathbf{x}^T \mathbf{Q} \mathbf{x} + \mathbf{p}^T \mathbf{x} \\ \text{subject to} \quad & \mathbf{A} \mathbf{x} = \mathbf{b} \\ & \mathbf{F} \mathbf{x} \leq \mathbf{g} \end{aligned} \quad (4.5)$$

where  $\mathbf{x}$  is the unknown variable and  $\mathbf{Q}$ ,  $\mathbf{p}$ ,  $\mathbf{A}$ ,  $\mathbf{b}$ ,  $\mathbf{F}$ ,  $\mathbf{g}$  are corresponding matrices in MPC and QP problem. The solution for this problem can be obtained by an available software; for example `cvx` [29].

**Remark 2:**

The integration is implemented by defining the terminal input-output constraints in the MPC problem with the purposes of driving the inputs-outputs converge to the optimum input-output targets from the upper layer. The convergence properties have not been proved formally. The complete integration approaches should be concerned in the future work.

### 4.3 Application to Distillation Column

In this section, we apply the two proposed integration approaches for the distillation column model. The comparisons of two approaches are illustrated through two aspects: the transient responses in the nominal case, the stability test responding to the change of one parameter in the RTO layer. First, we survey the transient responses of the closed loop system as some parameters vary to chose the most suitable parameters. The distillation column model ( $G_0$ ) in chapter 3 is used in the simulation. One of the inputs in the dynamic model, the reflux ratio  $R = L/D$ , is a variable from the RTO layer. Hence, in the MPC problem formulation (as Eq. 2.11), the reflux ratio  $R$  is included in the objective function as the input element. The degree of freedom of the system reduces to 1, which is the remaining input  $V$ , that will drive the output target, (bottom composition  $X_b$ ), converge to its optimum value (as in Table 2.2). The remaining output, distillate composition  $X_d$ , is restricted in the specific constraint.

#### 4.3.1 Tuning Parameters

In this task, some of parameters of the MPC controller are varied to determine the most efficiency one. The results from the Fig. 4.4, 4.5 and 4.6 show that: the parameters ( $N_p = 10$ ;  $N_c = 3$ ;  $\lambda = 1$ ) give the output responses of  $X_b$  with the small of the performancen index according to the *Integrated Absolute Error* (IAE) criterion. Hence, that parameters are chosen in the remaining of the chapter.

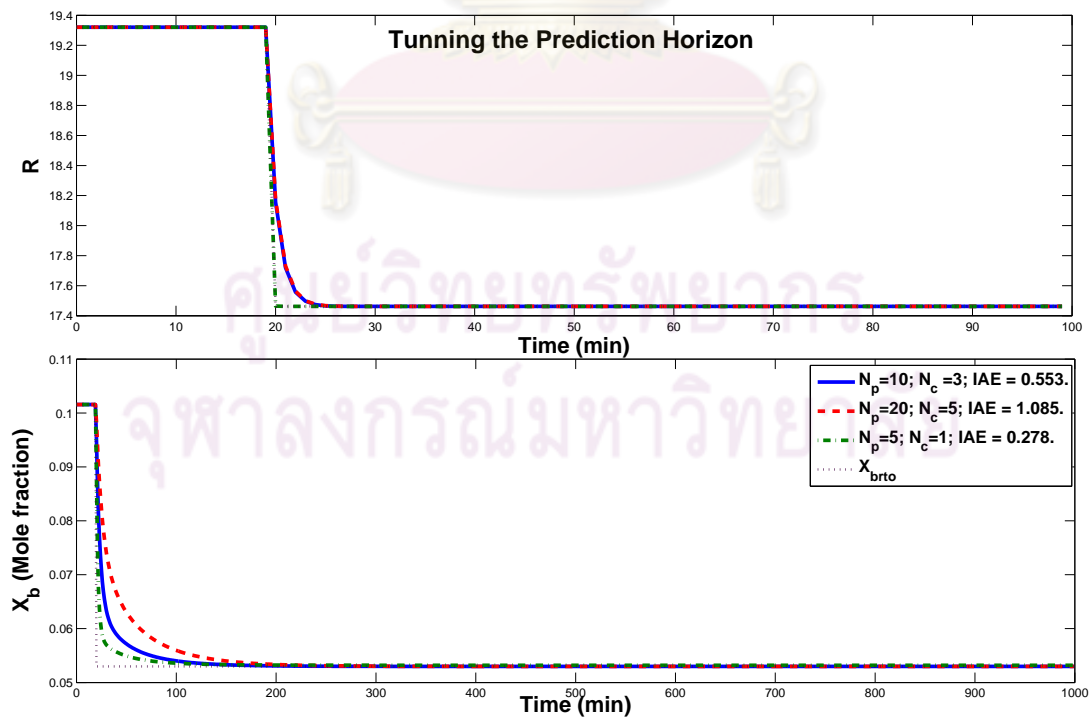


Figure 4.4: The transient responses of system output  $X_b$  and input  $R$  of the 2-layer as the prediction horizon varies.

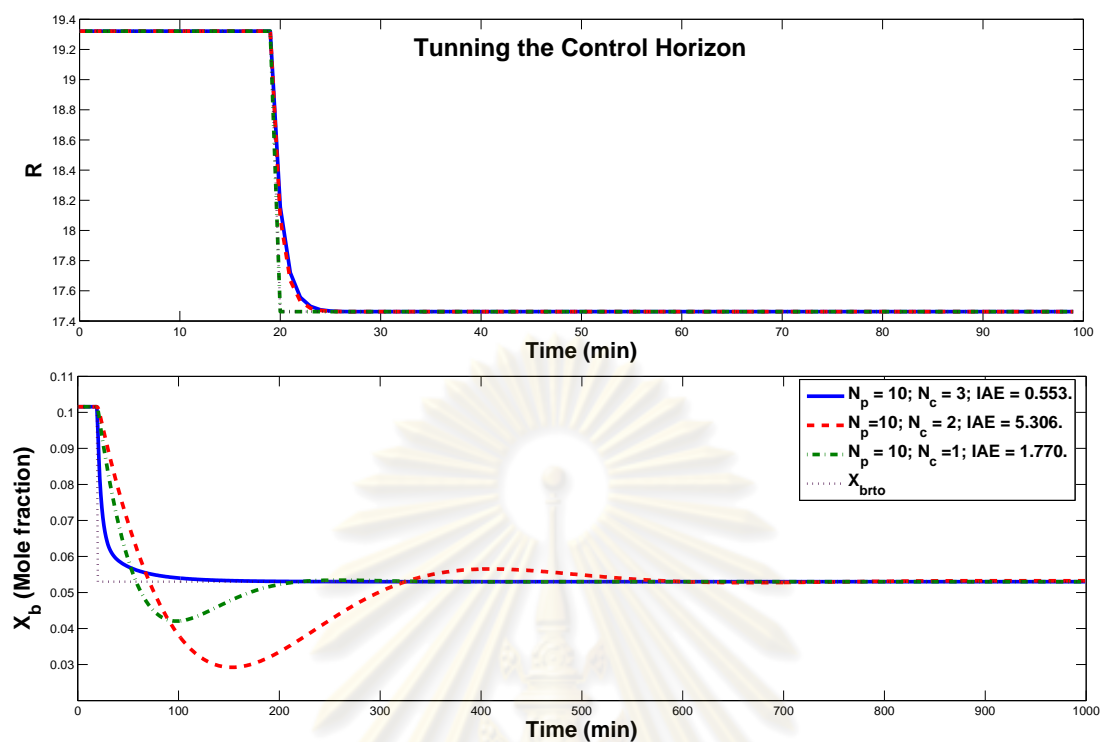


Figure 4.5: The transient responses of system output  $X_b$  and input  $R$  of the 2-layer as the control horizon varies.

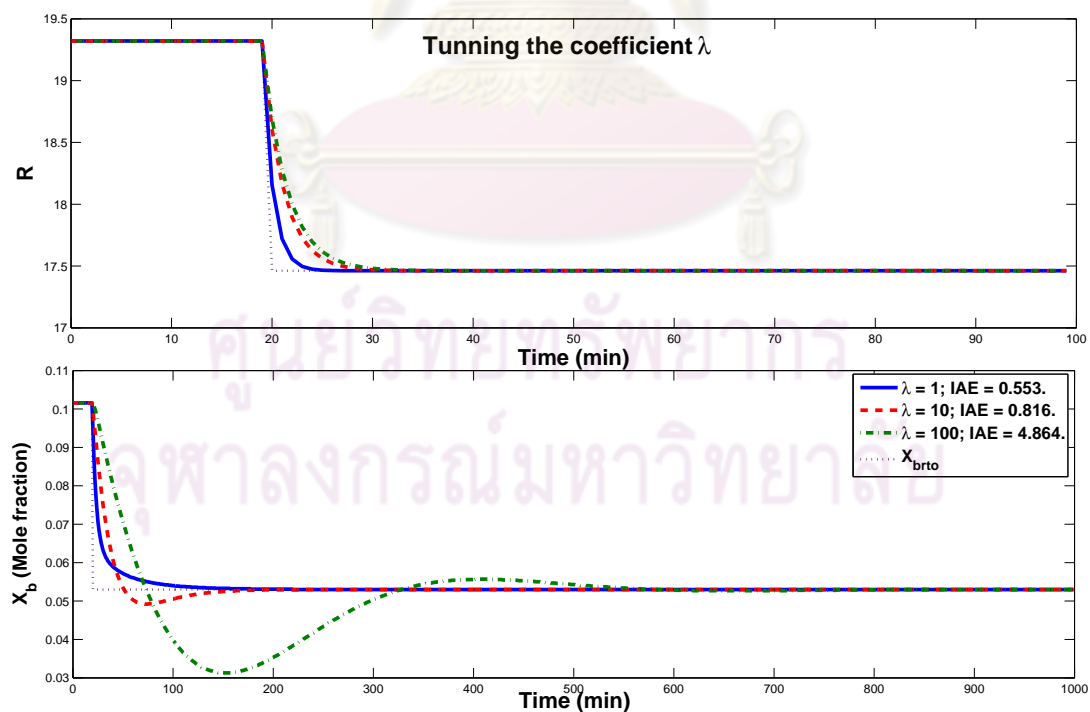


Figure 4.6: The transient responses of system output  $X_b$  and input  $R$  of the 2-layer as the weighting coefficient varies.



### 4.3.2 Transient Responses

#### Design Algorithm and Parameters for Simulation

- Step 1.* Starting from the nominal values in Table 3.1 [17] and the parameters in Table 2.1 [22]; the RTO problem for the distillation column is solved to compute the optimum input-output targets ( $R_{\text{rto}}$ ,  $X_{\text{brto}}$ ) as in Table 2.2 for the control layer ( $T_{\text{rto}} = 200$  min).
- Step 2.* The RTO layer transfers the optimum input-output targets to the control layers (QP of 3-layer, MPC of 2-layer). The controllers then compute the set-points for the process based on the linear model. The sampling periods of the controller are  $T_{MPC} = T_{QP} = 1$  min. During the first time interval of the RTO layer, the transient response of the distillation column is obtained.
- Step 3.* After 200 min, the RTO layer updates the data from the process. It is assumed that the parameter  $C_1$  in the utility cost (Eq. 2.2) varies to a new value which affects to the economic objective function in the RTO layer. The solution of the RTO problem gives the new targets for the control layers.
- Step 4.* In the second sampling period of the RTO layer, the step two is repeated and the transient responses of the distillation column are changed to converge into the new set-points.

*RTO layer:* is simulated in two time intervals with  $T_{\text{rto}} = 200$  min. The 1<sup>st</sup> time interval (21<sup>st</sup> - 200<sup>th</sup> min):  $C_1 = 6 \cdot 10^{-6}$  (\$/Btu), the solutions of the RTO problem give  $R_{\text{rto}} = 17.444$  and  $X_{\text{brto}} = 0.054$  (see Table 2.2).

The 2<sup>nd</sup> time interval (201<sup>st</sup> - 400<sup>th</sup> min):  $C_1 = 9 \cdot 10^{-6}$  (\$/Btu), the data from the process is updated at the first minute of the second time interval. The solution of the RTO problem gives  $R_{\text{rto}} = 16.62$  and  $X_{\text{brto}} = 0.073$  (see Table 2.2).

*MPC layer and QP layer:* the maximum inputs and maximum outputs are restricted in the allowable ranges as defined in chapter 3. The parameters for the controllers are chosen after several iterations.

The 2-layer and 3-layer structure

$$Q = \begin{bmatrix} 0 & 0 \\ 0 & 1 \end{bmatrix}; \quad E = \begin{bmatrix} 1 & 0 \\ 0 & 0 \end{bmatrix}; \quad S = \begin{bmatrix} 1 & 0 \\ 0 & 1 \end{bmatrix}; \quad P = \begin{bmatrix} 1000 & 0 \\ 0 & 1000 \end{bmatrix}; \quad N_p = 10, \quad N_c = 3; \quad T_{MPC} = T_{QP} = 1 \text{ min.}$$

- The 3-layer structure

$$Q_y = Q_u = \begin{bmatrix} 1 & 0 \\ 0 & 1 \end{bmatrix}; \quad C_\epsilon = \begin{bmatrix} 1000 & 0 \\ 0 & 1000 \end{bmatrix}.$$

Fig. 4.7 and Fig. 4.8 show that both proposed integration systems ensure the stability for the system after some sampling periods. It is illustrated by the convergence of the responses toward to their targets. The cost functions of two structures asymptotically decrease to 0 in Fig. 4.9.

Due to the addition of the QP layer, the input responses of the 2-layer structure have higher overshoots in comparison with those of the 3-layer one (Fig. 4.7). The cost function of the MPC layer (3-layer structure) is splitted with the QP layer, hence its peak is smaller than that of the 2-layer structure. As the cost function of the QP layer (3-layer structure) decreases to 0, the cost function of the MPC layer starts to decrease (Fig. 4.9). The Fig. 4.10 shows that the economic objective functions of two structures are similar to each other.

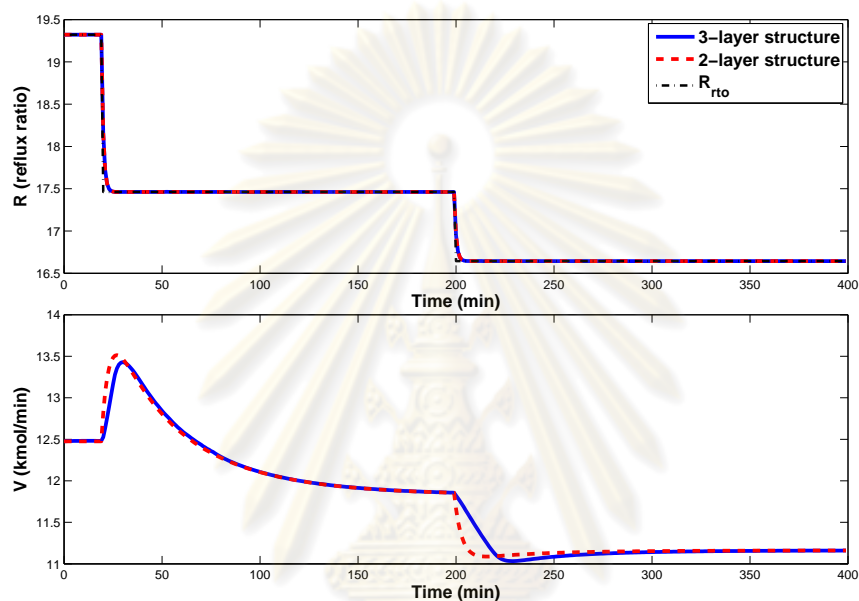


Figure 4.7: The system inputs of the 2-layer, 3-layer structure.

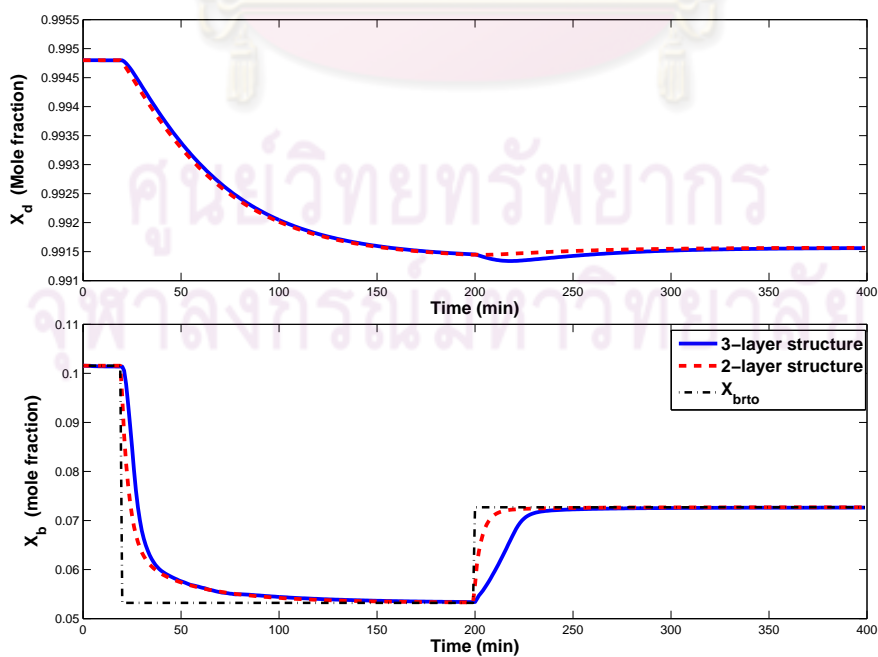


Figure 4.8: The transient responses of system outputs of the 2-layer, 3-layer structure.

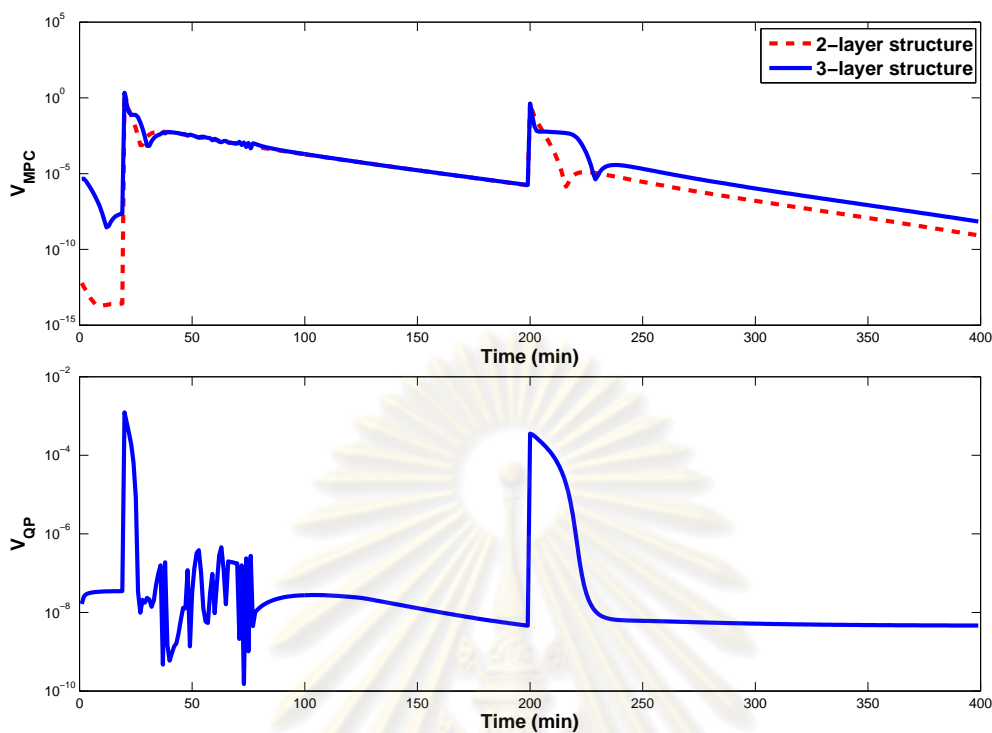


Figure 4.9: Cost functions in MPC layer and QP layer of the 2-layer and 3-layer structure.

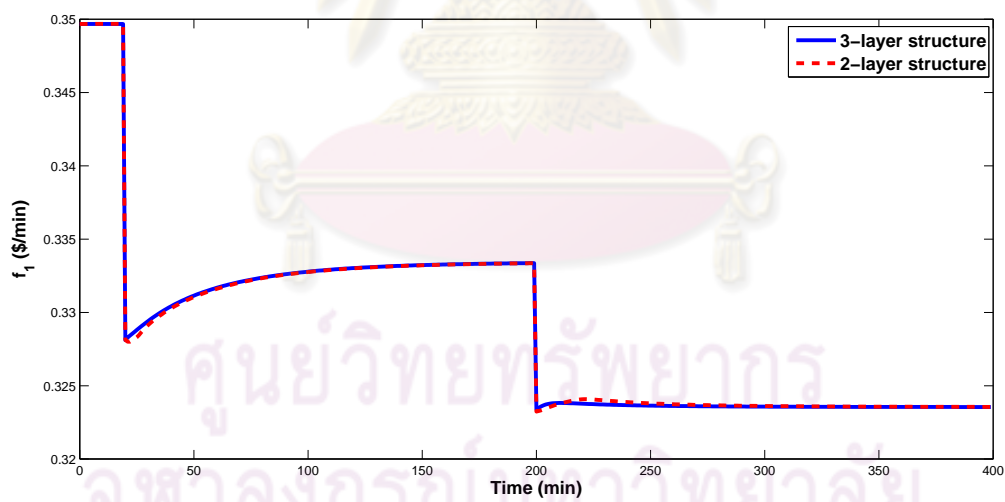


Figure 4.10: Economic objective functions (after omitting the raw material cost):  $C_1$  varies from  $6 \times 10^{-6}$  to  $9 \times 10^{-6}$  (\$/Btu) after the first 200<sup>th</sup> min.

### 4.3.3 Stability Test

In this task, the difference of two integration approaches and the effect of the prediction horizon length are evaluated in two aspects.

♣ *Finding the maximum allowable range of parameter  $C_1$  in the utility cost of the RTO layer.*

Assume that from 21<sup>th</sup> to 200<sup>th</sup> min,  $C_1 = 3 \times 10^{-6}$  \$/Btu. In this task, the previous MPC controllers and the new MPC controllers with ( $N_p = 20$ ,  $N_c = 5$ ) are used to find the maximum allowable range of  $C_1$  which still ensures the stability of the system after the first 200<sup>th</sup> minutes in three cases of the restriction in the rate of inputs.

- *Case 1:*  $\Delta u = 3\%$
- *Case 2:*  $\Delta u = 4\%$
- *Case 3:*  $\Delta u = 6\%$

The results in the table 4.1 shows that: the 3-layer structure has larger feasible domain in comparison with that of the 2-layer structure. Generally, as the prediction horizon increases, the feasible domain also enlarges.

Table 4.1: Maximum allowable  $C_1 (\times 10^{-6} \text{ \$/Btu})$ .

Case	$N_p = 10, N_c = 3$		$N_p = 20, N_c = 5$	
	2-layer	3-layer	2-layer	3-layer
1	4	17	8	17
2	6	17	15	17
3	11	17	17	17

The simulation result for the case 2, with the MPC controllers ( $N_p = 10$ ,  $N_c = 3$ ) response to  $C_1 = 10 \times 10^{-6}$  \$/Btu, is shown in Figure 4.11. As can be seen, the MPC controller of 2-layer structure gives the outputs responses exceed their bounds, those of the 3-layer structure are still inside the bound conditions and track to the target  $X_{brto}$ .

♣ *Wave Setpoints Trajectory.*

In this test, the wave setpoints trajectory with reference of input-output oscillates between two points: minimum  $R_{rto}$  ( $X_{bref} = 0.124$ ;  $R_{bref} = 15.456$ ) and maximum  $R_{rto}$  ( $X_{bref} = 0.032$ ;  $R_{bref} = 19.022$ ) is used. The 4 MPC controllers above are still be used. The maximum rate of inputs over the magnitude of inputs which allow the controllers guarantee the inputs, outputs in the allowable range and tracks to the setpoints are as follows.

Table 4.2: Maximum Rate of Inputs over Its Magnitude.

Case	$N_p = 10, N_c = 3$		$N_p = 20, N_c = 5$	
	2-layer	3-layer	2-layer	3-layer
	0.07	0.001	0.04	0.001



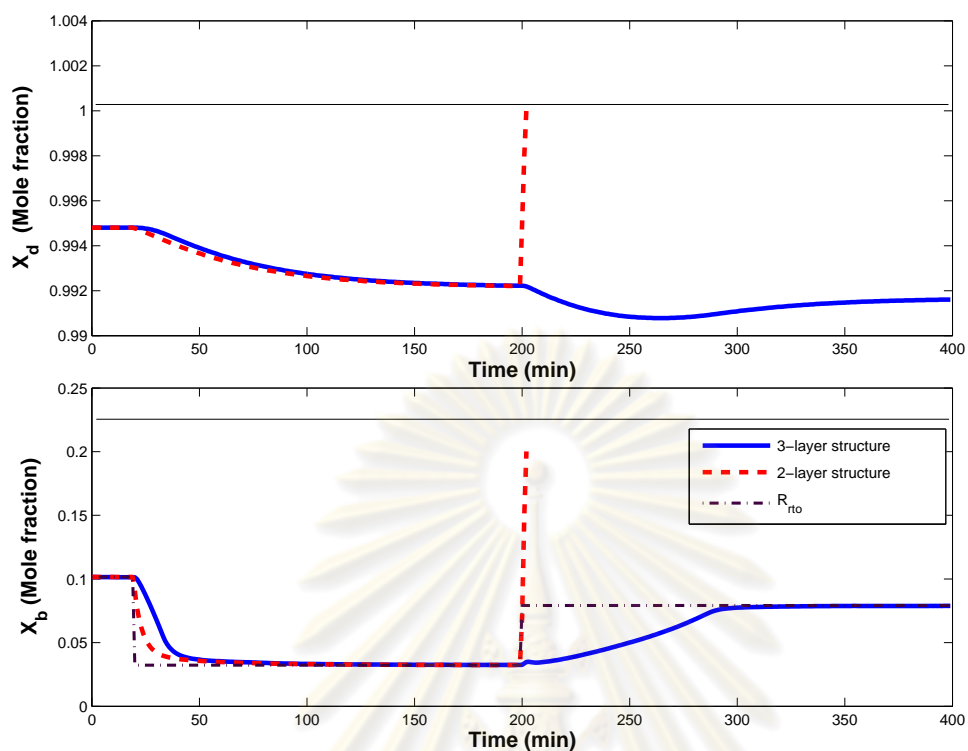


Figure 4.11: The output responses of the nominal integration approaches (2-layer and 3-layer structure) as the parameter  $C_1$  (RTO layer) varies from  $3 \times 10^{-6}$  \$/Btu to  $10 \times 10^{-6}$  \$/Btu after the first 200<sup>th</sup> min; ( $N_p = 10$ ,  $N_c = 3$ ) (case 2).

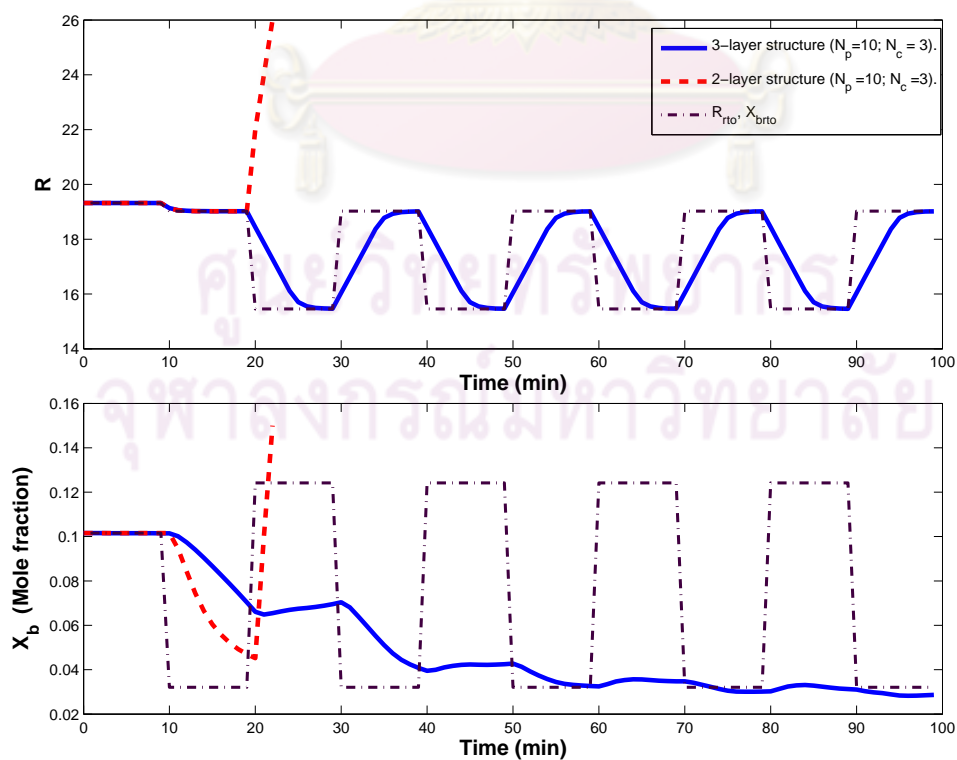


Figure 4.12: The input  $R$ -output  $X_b$  responses of the nominal integration approaches (2-layer and 3-layer structure) ( $N_p = 10$ ,  $N_c = 3$ ) as the limitations rate of input is 0.03



## CHAPTER V

### INTEGRATION OF RTO AND MULTIPLE MPC

#### 5.1 Introduction

In this chapter, the integration approaches (3-layer and 2-layer structure) for the uncertain systems are proposed. The RTO problem for the rigorous model is similar to the nominal case. The difference is in the assumption that the dynamic model for the control layers varies in the finite set of models (*multiple models*). Each element in the set corresponds with each operating point of the process which is well-described by a linear-state space model. The motivation

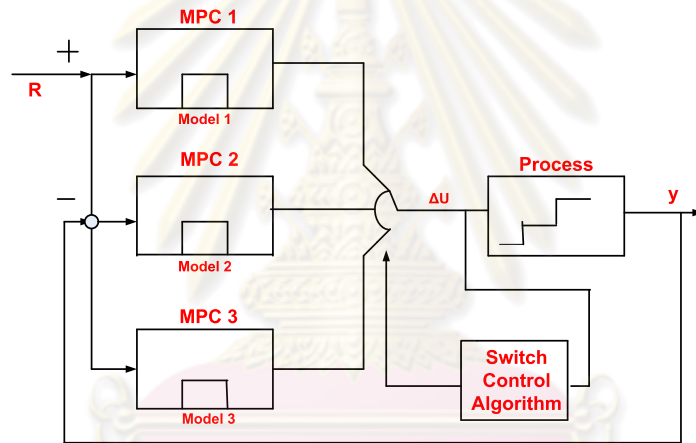


Figure 5.1: The output-feedback MPC controller for the distillation column based on the multiple models using the switching scheme.

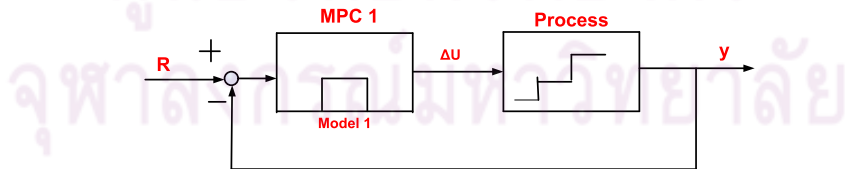


Figure 5.2: The output-feedback nonadaptive MPC controller for the distillation column based on single model.

of the multiple models approach comes from the fact that, normally, the controller being designed to control the process based on the assumption of nominal models and neglecting all internal and external uncertainties. It simplifies MPC formulation dramatically, but may impair the controller performance and/or the closed-loop stability. In practice, as a linear

controller is applied to control a nonlinear process, it is limited to relatively small operating regions. The accuracy of the process model has a significant effect on the performance of the closed-loop system for those being designed bases entirely on model prediction [30].

An approach is to divide the process into several operating regions, each region is approximated by a linear model. The control strategies, which are based on multiple models, have appeared in the control literature in three different contexts [31]: *Model scheduling strategy*, *Adaptive control scheme* and *Robust control strategy*. In this thesis, we apply one of the adaptive control scheme based on multiple models in designing the controller for distillation columns: multiple MPC switch controller as in Fig. 5.1. The switching methodology is motivated from Ciprian [32] with some modifications, specifically the reflux ratio  $R$  is chosen as the variable to indicate which controller-model pair is active. Subsequently, the integration of the RTO and multiple MPC with 3-layer and 2-layer structure are formulated. Then, the obtained integration foundations are used to control the distillation column (being described by 3 models  $G_0$ ,  $G_1$ ,  $G_2$  chapter 3-section 2).

The switching control method is used in the design based on the values of the input reflux ratio  $R$  at the corresponding sampling instant. The advantage of this approach is that it maintains the performance of the controller over wide range of the operating levels; whereas, the wealth of design and tuning strategies for the linear controllers can used [32]. On the contrary, as a controller designed bases on the nominal model around the nominal operating point, once the process changes to another operating condition, the mismatch between the process and the model probably degrades or damages the closed loop systems's performance and stability.

To compare the results of the multiple MPC controllers, the nonadaptive MPC controllers with output feedback are implemented in parallel with the integration of RTO and multiple MPC approaches.

### The Switching Control Algorithm

1. The MPC controller 1 is chosen, starting from the nominal model  $G_0$ . That controller-model pair is chosen as the deviation of the input reflux ratio  $R$  in the range of  $-1.85 \leq \Delta R \leq 3.865$  (Corresponding with the maximum deviation of  $R$  until  $R = R_1 = 17.46$  (chapter 3)).
2. As  $-2.65 \leq \Delta R \leq -1.85$ , the controller-model pair 1 is chosen with  $G = G_1$ . That range corresponds with  $R = R_1 = 17.46$  until  $R = R_2 = 16.64$ .
3. As  $-3.85 \leq \Delta R \leq -2.65$ , the controller-model pair 2 is chosen with  $G = G_2$ . That range corresponds with  $R = R_2 = 16.64$  until  $R = R_{\min} = 15.54$ .

All the data of the process models can be found in chapter 3.

## 5.2 Integration of RTO and Multiple MPC

Generally, the integration approaches and the RTO problem formulation are similar to the nominal case in chapter 4. What are the main differences between the integration approaches of this chapter with the integration based on the nominal model in chapter 4? First, there are multiple models being used for describing the process (distillation column) in several operating points. Second, the MMPC is used in the design for the dynamic models. The controller-model pair is switched in each pair as the function of the manipulated variable  $R$ .

### 5.2.1 The 2-layer structure approach

The Fig. 5.3 (A) illustrates the integration of RTO and multiple MPC in 2-layer structure. As can be seen, the RTO layer transfers target to the MPC controller. The MPC controller designed bases of the each model is selected as the function of the manipulated variables, the reflux ratio  $R$ . The simulation results of this integration approaches for the distillation column are in section 5.4.

The RTO problem of the distillation column has been formulated and solved in chapter 2. The MPC problem with input-output tracking targets are formulated based on a prediction model as the MPC problem based on the nominal model in chapter 2. The difference with the nominal case (chapter 4) is that there are 3 models taken in the design. In this chapter, we only illustrate the results of the integration approaches through the distillation column application and will not repeat the problem formulation.

### 5.2.2 The 3-layer structure approach

The Fig. 5.3 (B) illustrates the integration of RTO and multiple MPC in 3-layer structure. The QP layer is added to recompute the targets for the MPC controller. The remaining parts are similar to the 2-layer approach above.

## 5.3 Application to Distillation Column

In this section, the integration of the 2-layer and 3-layer structures based on multiple MPC are used to do the simulations based on the distillation column model. In accordance with that, the nonadaptive model predictive control strategies (the MPC control strategy based on the nominal model/the process varies) are implemented to illustrate the efficiency of the multiple MPC strategies.

### 5.3.1 Tuning Parameters

The simulations are implemented by varying the prediction horizon, the control horizon and the coefficient  $\lambda$  of the weighting matrix in the input element of the MPC cost function. We also use the *Integrated Absolute Error* (IAE) criterion to evaluate the transient responses of

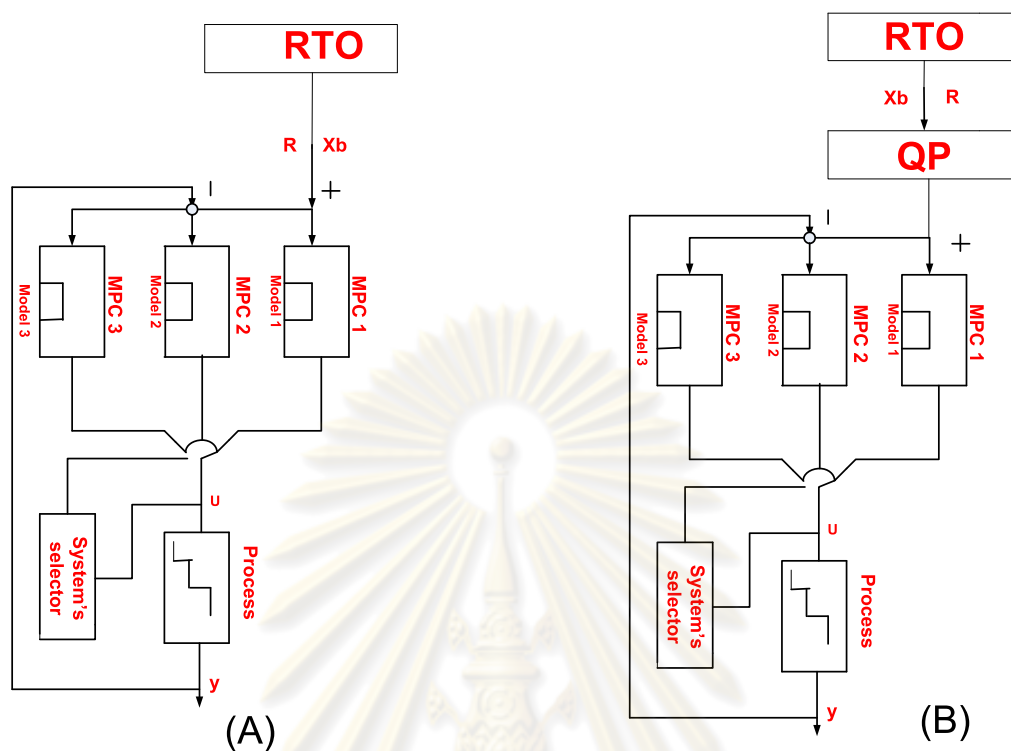


Figure 5.3: The integration structure of RTO and multiple MPC: (A) 2-layer approach and (B) 3-layer approach.

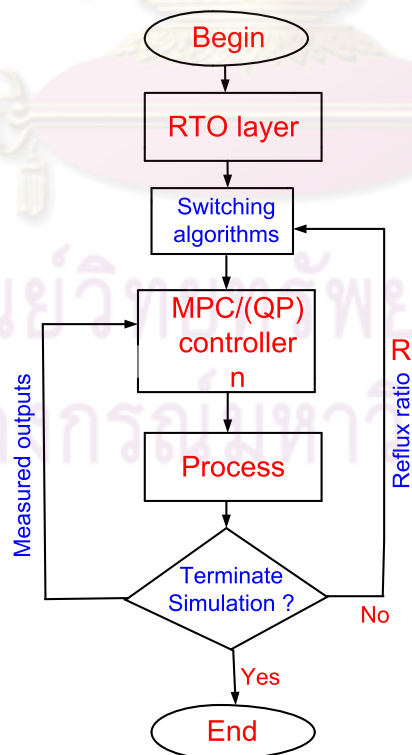


Figure 5.4: The design algorithm of the integration RTO and multiple MPC based on switch controller.

each controller. The simulations shows that the MPC controller with ( $N_p=10$ ;  $N_c=3$ ;  $\lambda=1$ ) gives the smallest IAE index. Thus, we chose that parameters for doing simulations in next sections.

### 5.3.2 Transient Responses

- Choosing Parameters *RTO layer*: is simulated in two time intervals with  $T_{rto} = 200$  min.
  - 1<sup>st</sup> time interval (21<sup>st</sup> - 200<sup>th</sup> min):  $C_1 = 6 \cdot 10^{-6}$  (\$/Btu), the solutions of the RTO problem give  $R_{rto} = 17.46$  and  $X_{brto} = 0.053$  (see Table 2.2).
  - 2<sup>nd</sup> time interval (201<sup>st</sup> - 400<sup>th</sup> min):  $C_1 = 9 \cdot 10^{-6}$  (\$/Btu), the data from the process is updated at the first minute of the second time interval. The solution of the RTO problem gives  $R_{rto} = 16.64$  and  $X_{brto} = 0.073$  (see Table 2.2).
- *MPC layer and QP layer*: the maximum inputs and maximum outputs are restricted in the allowable ranges as defined in section 3.2. The parameters for the controllers are chosen as chapter 4.

- The 2-layer

$$Q = \begin{bmatrix} 0 & 0 \\ 0 & 1 \end{bmatrix}; \quad E = \begin{bmatrix} 1 & 0 \\ 0 & 0 \end{bmatrix}; \quad S = \begin{bmatrix} 1 & 0 \\ 0 & 1 \end{bmatrix}; \quad P = \begin{bmatrix} 1000 & 0 \\ 0 & 1000 \end{bmatrix}; \quad N_p = 10, N_c = 3;$$

$$T_{MPC} = T_{QP} = 1 \text{ min.}$$

- The 3-layer structure

$$Q_y = Q_u = \begin{bmatrix} 1 & 0 \\ 0 & 1 \end{bmatrix}; \quad C_\epsilon = \begin{bmatrix} 1000 & 0 \\ 0 & 1000 \end{bmatrix}.$$

Fig. 5.8, 5.9 and 5.10 compare the responses of the 2-layer (adaptive, nonadaptive). Fig. 5.11, 5.12 and 5.13 compare the responses of the 3-layer (adaptive, nonadaptive) structure. The simulation results show that the output responses of adaptive approaches have smaller overshoot in comparison with that of the nonadaptive approaches. The reason is because the adaptive approach, as the process transfer from this operating regime to another operating regime, the MPC-model pair corresponds to the new regime is automatically updated. On the contrary, the nonadaptive approach, the MPC-model only used the nominal model around the nominal operating point even when the process has transferred into another operating regime.

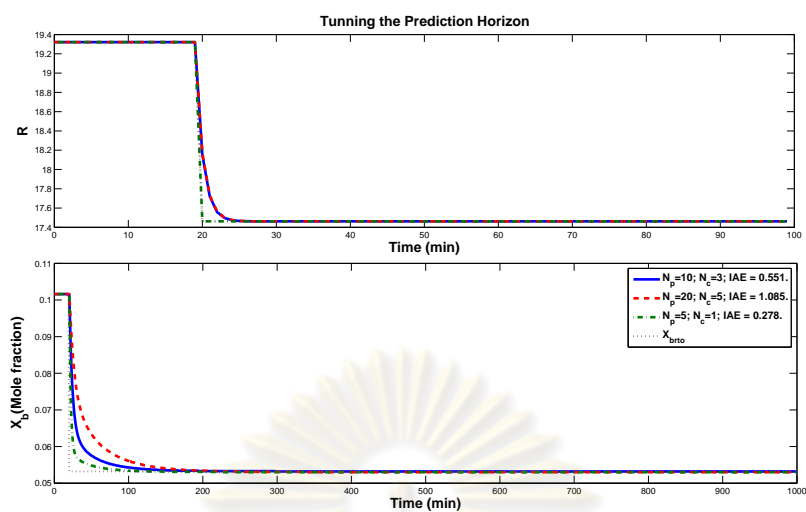


Figure 5.5: The transient responses of system output  $X_b$  and input  $R$  of the 2-layer as the prediction horizon varies.

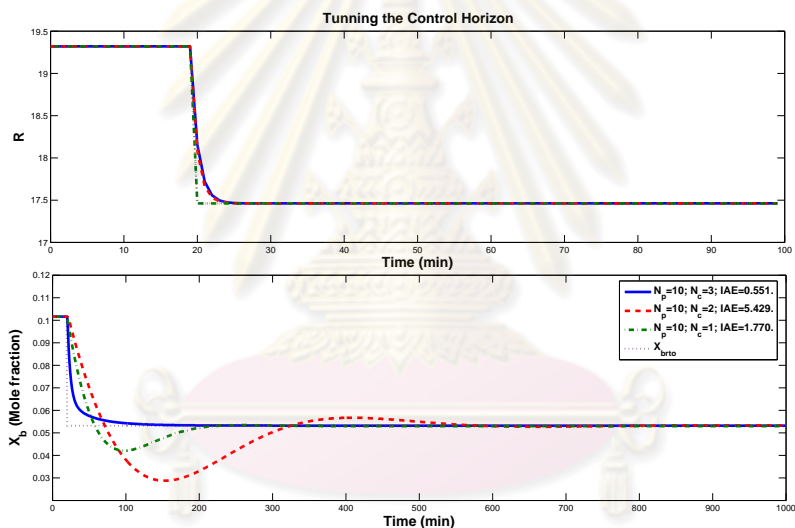


Figure 5.6: The transient responses of system output  $X_b$  and input  $R$  of the 2-layer as the control horizon varies.

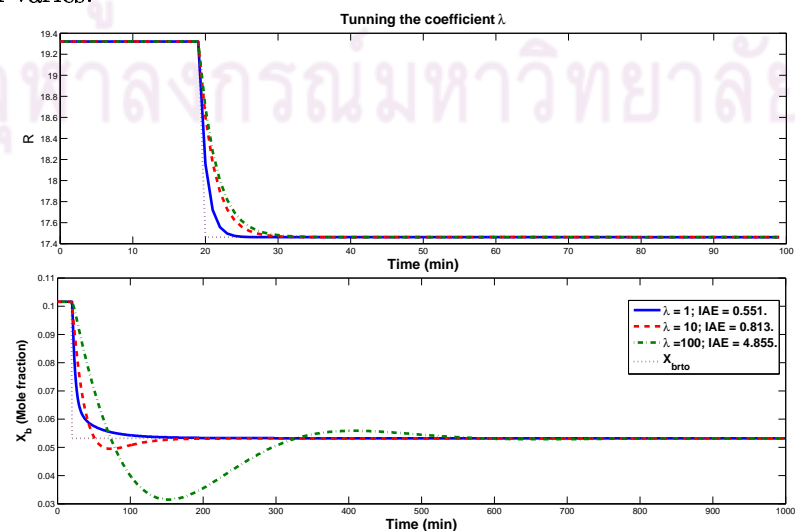


Figure 5.7: The transient responses of system output  $X_b$  and input  $R$  of the 2-layer as the weighting coefficient varies.



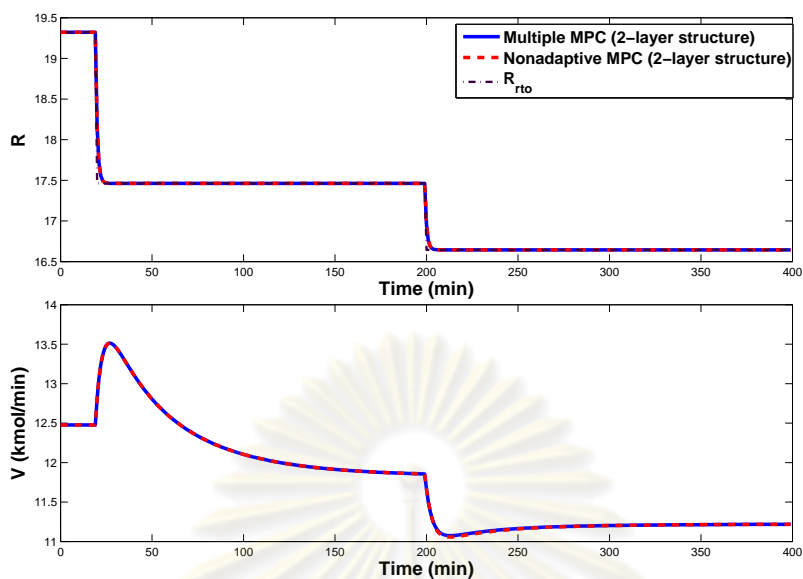


Figure 5.8: The MPC inputs of the nominal MPC and multiple MPC (2-layer structure).

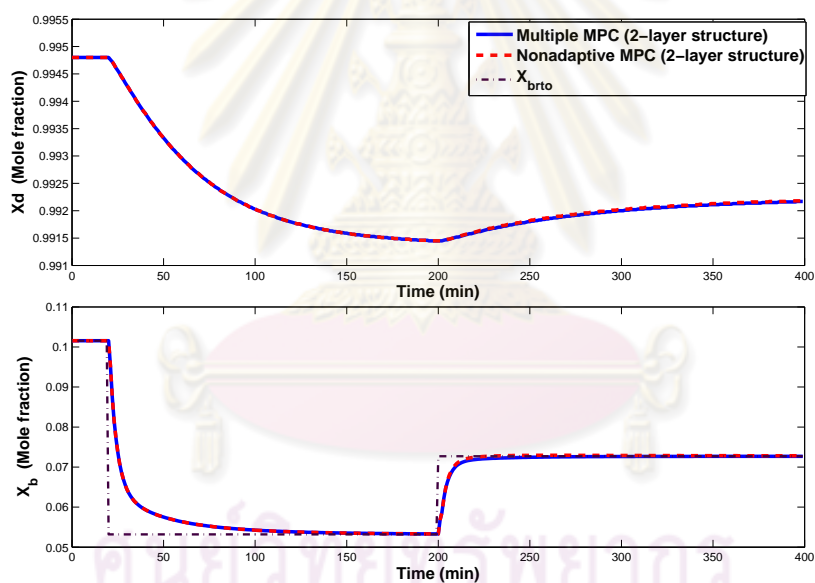


Figure 5.9: The MPC outputs of the nominal MPC and multiple MPC (2-layer structure).

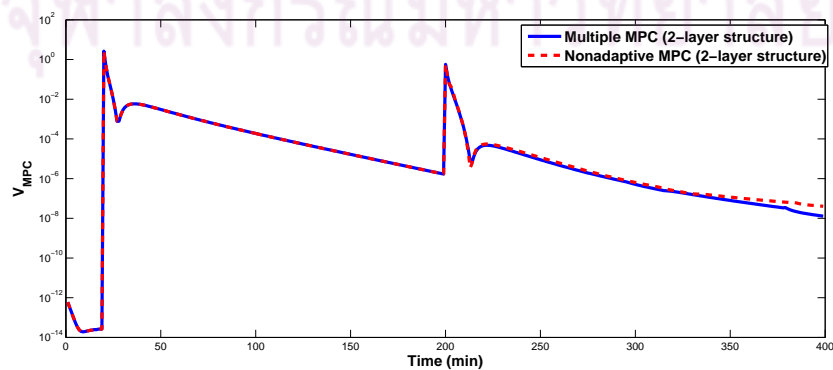


Figure 5.10: The cost of the nominal MPC and multiple MPC (2-layer structure).

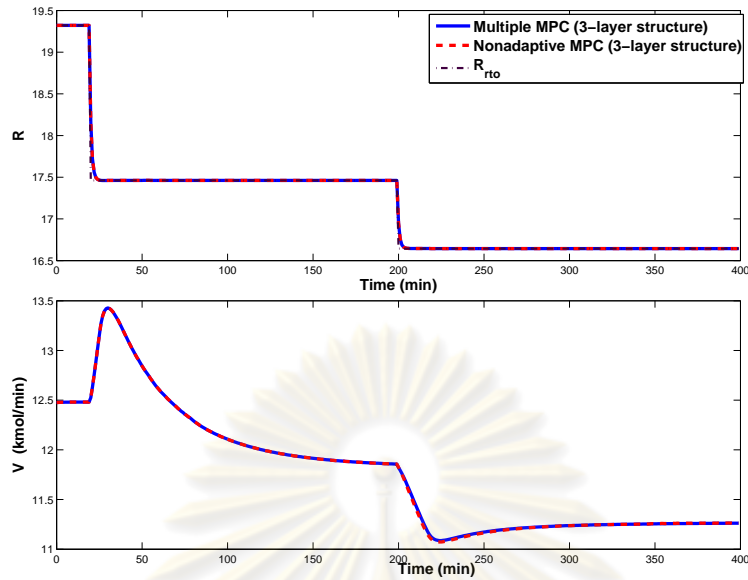


Figure 5.11: The MPC inputs of the nominal MPC and multiple MPC (3-layer structure).

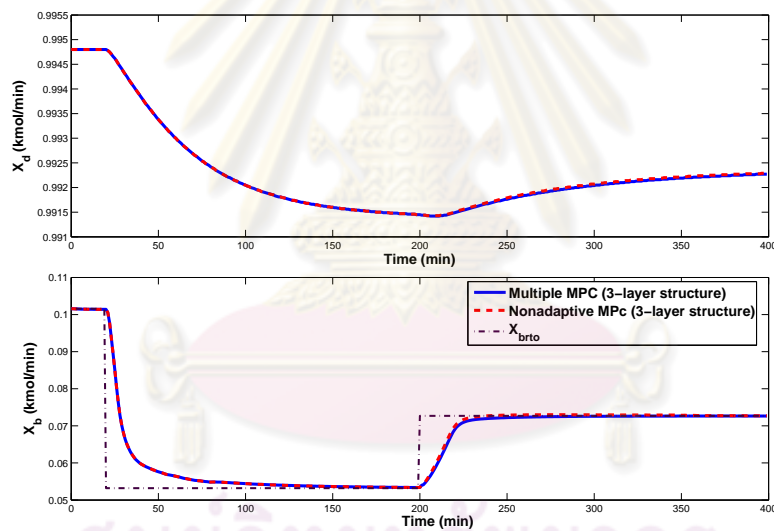


Figure 5.12: The MPC outputs of the nominal MPC and multiple MPC (3-layer structure).

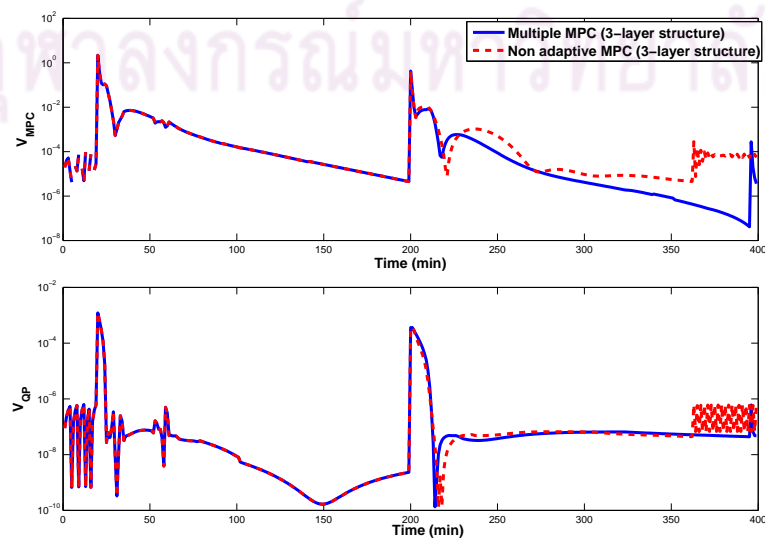


Figure 5.13: The cost of the nominal MPC and multiple MPC (3-layer structure).

### 5.3.3 Stability Test

♣ *Finding the maximum allowable range of parameter  $C_1$  in the utility cost of the RTO layer.*

Assume that from 21<sup>th</sup> to 200<sup>th</sup> min,  $C_1 = 3 \times 10^{-6}$  \$/Btu. In this task, the multiple MPC controllers ( $N_p = 10$ ,  $N_c=3$ ) and the multiple MPC controllers with ( $N_p = 20$ ,  $N_c = 5$ ) in 2-layer and 3-layer structures are used to find the maximum allowable range of  $C_1$  which still ensures the stability of the system after the first 200<sup>th</sup> minutes in three cases of the restriction in the rate of inputs.

- *Case 1:  $\Delta u = 3\%$*
- *Case 2:  $\Delta u = 4\%$*
- *Case 3:  $\Delta u = 6\%$*

The results in the table 5.1 shows that: the 3-layer structure has larger feasible domain in comparison with that of the 2-layer structure. Generally, the prediction horizon increases, the feasible domain is enlarged.

Table 5.1: Maximum allowable  $C_1 (\times 10^{-6} \$/\text{Btu})$ .

Case	$N_p = 10, N_c=3$		$N_p = 20, N_c=5$	
	2-layer	3-layer	2-layer	3-layer
1	6	17	11	17
2	8	17	17	17
3	14	17	17	17

The simulation result for the case 2, with the multiple MPC controllers (2-layer, 3-layer structure) and ( $N_p = 10$ ,  $N_c=3$ ) responses to  $C_1 = 10 \times 10^{-6}$  \$/Btu, is shown in Fig. 5.14. As can be seen, the MPC controller of 2-layer structure gives the outputs responses exceed their bounds, those of the 3-layer structure are still inside the bound conditions and track to the target  $X_{brto}$ .

♣ *Wave Setpoints Trajectory.*

In this task, the comparison of the integration approaches based multiple MPC and nonadaptive MPC (2-layer structure) are evaluated by wave reference trajectories [33]. We assume that the setpoints oscillate between two points: maximum  $R_{rto}$  ( $R=19.022$ ,  $X_b=0.032$ ) and minimum  $R_{rto}$  ( $R=15.456$ ,  $X_b=0.124$ ). The simulation results (Fig. 5.15) confirm that the multiple MPC gives better transient responses in comparison with that of the nonadaptive MPC since its transient responses have less setting time and smaller overshoot in comparison with those of nonadaptive MPC.

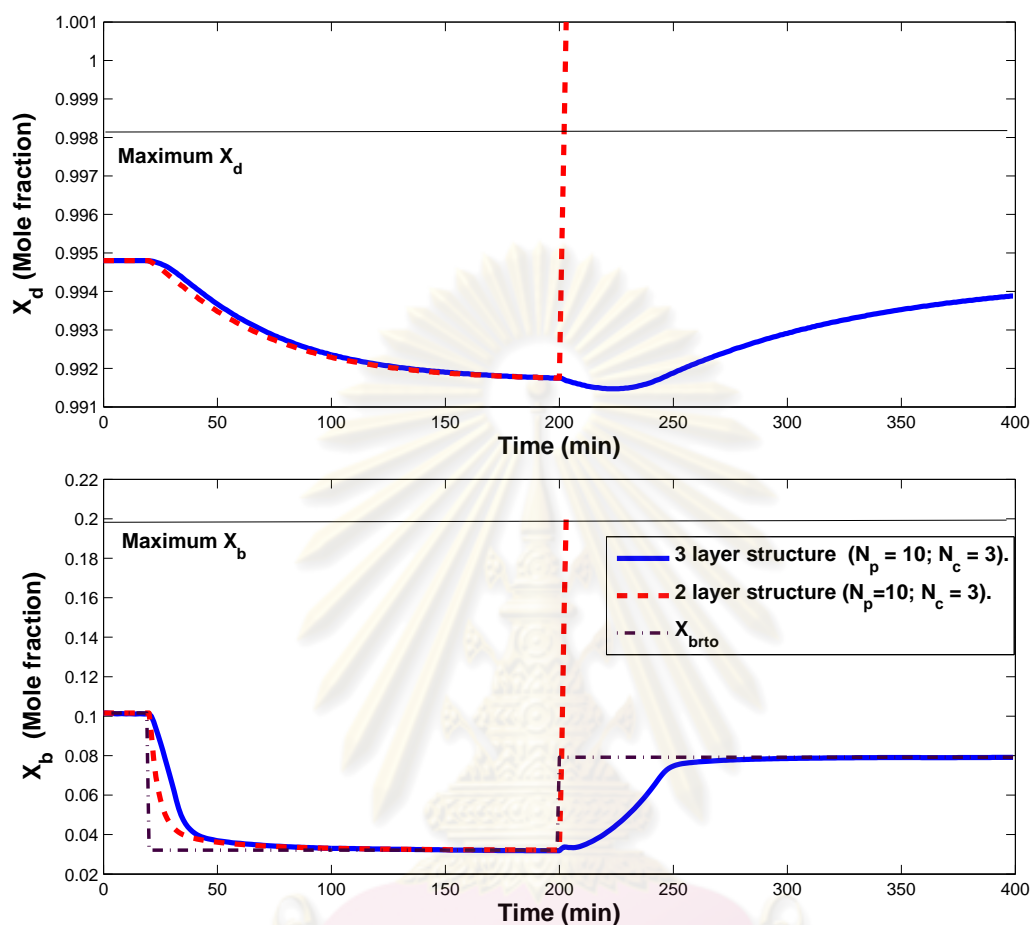


Figure 5.14: The output responses of the multiple integration approaches (2-layer and 3-layer structure) with ( $N_p = 10$ ,  $N_c = 3$ ) as the parameter  $C_1$  (RTO layer) varies from  $3 \times 10^{-6}$  \$/Btu to  $10 \times 10^{-6}$  \$/Btu after the first 200<sup>th</sup> min (case 2).

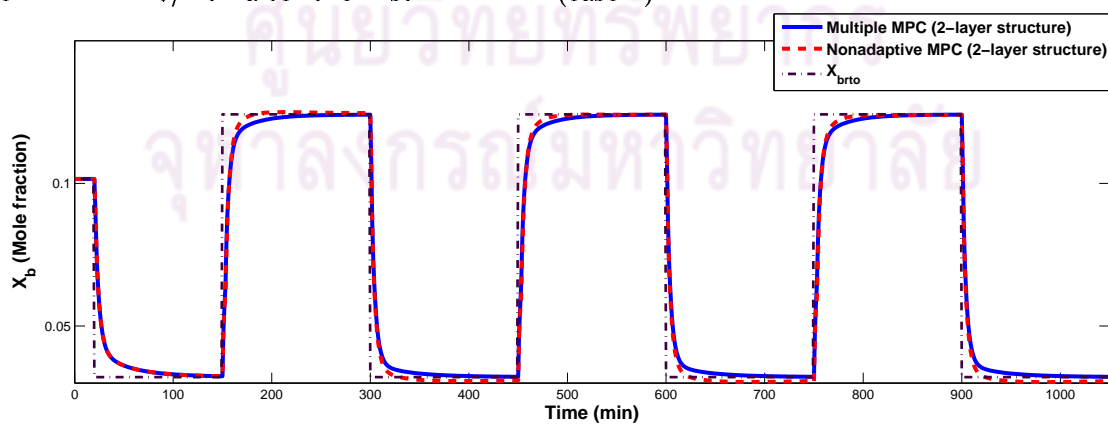


Figure 5.15: The output responses with the wave reference trajectory of the 2-layer structure.

## 5.4 Conclusion

In this chapter, the integration of RTO and multiple MPC have been introduced and applied for the distillation column. There are some points that differs to the nominal case (chapter 4). First, the system is described separately in several regimes depending on the value of the reflux ratio  $R$  that is transfered from the RTO layer. Second, the multiple MPC based multiple models using switching algorithm is implemented according to the predefined algorithms.

The simulation results of the application to the distillation column demonstrate the wealth of the controller design based on the multiple models in comparisons with the controller based on the nominal model. Specifically, the responses of the multiple controllers have less overshoot and smaller setting time compared with that of the nominal (nonadaptive) controller.



# CHAPTER VI

## CONCLUSIONS

### 6.1 Summary of Results

In this thesis, we propose the integration approaches of Real Time Optimization (RTO) and Model Predictive Control (MPC) and their applications to distillation column. Chapter 1 presents the literature review about the integration RTO and MPC in literature. We have reviewed the integration of RTO and MPC layer in 1-layer, 2-layer and 3-layer structure. Subsequently, the motivation of the integration RTO and MPC in 3-layer structure by using finite horizon MPC is derived. The survey about RTO and MPC control problems for the distillation column are also implemented. Subsequently, the propylene-propane (a kind of distillation column) is chosen to implement the simulations.

Chapter 2 presents the basic knowledge about Real Time Optimization and Model Predictive Control. We also formulate and solve the RTO problem for the propylene-splitter and the finite horizon MPC problem with input-output tracking targets.

Chapter 3 constructs the dynamic models of the distillation column. Based on the Skogestad's method [27], the dynamic models of the distillation column are obtained from a series of equations which describe the operation of the distillation column. The data of this distillation column comes from model D ([17]). As a result, one obtains 3 models which describe the process in 3 distinguished operating points. That models will be used in the simulation of the integration approaches for comparison.

Chapter 4 introduces the integration of RTO and finite horizon MPC. The RTO problem of the distillation column (a propylene splitter) is formulated and solved from a specific economic objective function. The solutions give the targets for the MPC controller (reflux ratio  $R$  and bottom composition  $X_b$ ). Subsequently, the formulation of RTO and finite horizon MPC in 2-layer and 3-layer structure based on nominal model are provided. The objectives of the formulations are to guarantee that the (MPC) controller drives the variables track to the targets from RTO layer. The added QP layer in the 3-layer structure recomputes the targets for the MPC layer. The differences of 2 integration approaches are illustrated in the distillation column applications. It is shown that the transient responses of 2-layer structure are faster than that of 3-layer structure. On the contrary, the 3-layer structure provides a larger feasible domain for the varying of a variable in the RTO layer due to the addition QP layer.

Chapter 5 formulates the integration of RTO and multiple MPC. In this chapter, it is assumed that the process (distillation column) is described by a set of model (in stead of a



nominal model - chapter 4). The multiple MPC techniques has been shown to be effectively control the varying process. The formulation of integration RTO and multiple MPC is similar to the nominal case (chapter 4). The only difference locates in the switch controller being used in the design - that is used for the MPC controller. In this case, the controller- model pair is updated based on the measured variables of the process. The simulation results are repeated as in the nonadaptive case.

In summary, the main contributions of this thesis are to introduce the integration of RTO and MPC, RTO and multiple MPC in 3-layer structure, and their applications to the distillation column. The comparisons with the conventional 2-layer structures are evaluated in several aspects.

## 6.2 Conclusion

This thesis presents the integration of RTO and (nominal, multiple) MPC in 3-layer structure and their applications to the distillation column. The simulations illustrate the efficiency of the integration RTO and MPC in 3-layer structure in comparison with the 2-layer structure. The multiple MPC using the switching scheme illustrates its efficiency in comparisons with the nonadaptive one.

## 6.3 Recommendations for Future Works

1. The integration is implemented by defining the terminal input-output constraints in the MPC problem with the purposes of driving the inputs-outputs converge to the optimum input-output targets from the upper layer. The completed integration approaches should be concerned in the future work.
2. Make the comparison with other integration approaches which have been proposed in the literature and using other controllers. For example, the multiple MPC can be replaced by PI, LQR [34], min-max optimization MPC controller [31].
3. Develop the integration approaches for other applications. Since the integrations of RTO and MPC have been widely applied in practice for many chemical and integrated processes.
4. Develop the numerical methods for solving the RTO and MPC problems. In this thesis, the RTO problem of the distillation column is solved by MATLAB optimization toolbox. Whereas, the finite horizon MPC, which is formulated as QP problem, is solved by using `cvx` software. This is still an active area for developing the numerical methods of solving the optimization problems in this thesis.

## REFERENCES

- [1] V. A. Adetola. *Integrated Real Time Optimization and Model Predictive Control Under Parametric Uncertainties*. PhD thesis. Queen's University. Canada. 2008.
- [2] M. S. Govatsmark. *Integrated Optimization and Control*. PhD thesis. Norwegian University of Science and Technology, Norway. 2003.
- [3] L. Alvarez and D. Odloak. Robust integration of Real Time Optimization with linear Model Predictive Control. *Journal of Computers and Chemical Engineering*. 34. (2010): 1937-1944.
- [4] C. Ying and B. Joseph. Performance and stability analysis of the LP-MPC and QP-MPC cascade control systems. *AIChE Journal*. 45. 7. (1999): 1521-1534.
- [5] T. Tosukhowong and J. H. Lee. Real-time Economic Optimization for an integrated plant via a Dynamic Optimization Scheme. in *Proceeding of the 2004 American Control Conference*. (2004): 233-238.
- [6] J. Rawlings and R. Amrit. *Nonlinear Model Predictive Control*. ch. Optimizing process economic performance using Model Predictive Control, pp. 119–138. Lecture Notes in Control and Information Sciences. Springer-Verlag Berlin Heidelberg. 2009.
- [7] A. Zanin, T. Gouvea, and D. Odloak. Integrating Real Time Optimization into the Model Predictive Controller of the FCC system. *Journal of Control Engineering Practice*. 10. (2002): 819-831.
- [8] D. Souza, D. Odloak, and A. Zanin. Real Time Optimization with Model Predictive Control. *Computer Aided Chemical Engineering*. 27. (2009): 1365-1370.
- [9] J. Kadam, M. Schlegel, W. Marquardt, R. Tousain, D. Hessem, J. Berg, and O. Bosgra. A two-level strategy of integrated dynamic optimization and control of industrial processes - a case study. in *J. Grievink, J. V. Schijndel(Eds.): European Symposium on Computer Aided Process Engineering*. (2002): 511-516.
- [10] J. Kadam, W. Marquardt, M. Schlegel, T. Backx, O. Bosgra, P. Brouwer, G. Dunnebieer, D. Hessem, A. Tiagounov, and S. Wolf. Towards integrated dynamic Real Time Optimization and control of industrial processes. in *In Proc. Foundations of Computer Aided Process Operations (FOCAPO 2003)*. (2003): 593-596.
- [11] J. Kadam and W. Marquardt. *Assessment and Future Directions of Nonlinear Model Predictive Control*. vol. 358 of *Lecture Notes in Control and Information Sciences*.

ch. Integration of Economical Optimization and Control for Intentionally Transient Process Operation, pp. 419–434. Springer-Verlag Berlin Heidelberg, 2007.

- [12] V. Adetola and M. Guay. Integration of Real Time Optimization and Model Predictive Control. *Journal of Process Control*. 20. 2. (2009): 125-133.
- [13] M. Krstic and H. Wang. Stability of extremum seeking feedback for general nonlinear dynamic systems. *Automatica*. 36. (2000): 595-601.
- [14] H. Chen and Y. Lin. Case Studies on optimum Reflux Ratio of Distillation Towers in petroleum refining processes. *Tamkang Journal of Science and Engineering*. 4. 2. (2001): 105-110.
- [15] A. Torgashov, K. Park, H. Choi, and Y. Choe. Real-time Optimization of Distillation Column via Sliding Modes. in *Proc. 7th IFAC International Symposium on Advanced Control of Chemical Processes (ADCHEM7), Hong Kong*. vol. 2. (2004): 791-794.
- [16] Z. Ying, L. Wenxiang, H. Dexian, J. Yongheng, and J. Yihui. A new strategy of integrated control and online optimization on high-purity distillation process. *Chinese Journal of Chemical Engineering*. 18. 1. (2010): 66-79.
- [17] S. Skogestad and M. Morari. Understanding the Dynamic Behavior of Distillation Columns. *Journal of Industrial and Engineering Chemistry Research*. 27. 10. (1988): 1848-1862.
- [18] V. T. Minh and W. M. W. Muhamad. Model Predictive Control of a condensate Distillation Column. *International Journal of Systems Control*. 1. 1. (2010): 4-12.
- [19] J. Wallker and J. Boling. Multivariable nonlinear MPC of an ill-conditioned Distillation Column. *Journal of Process Control*. 15. 1. (2005): 23-29.
- [20] P. Grosdidier, B. Froisy, and M. Hammann. The IDCOM-M controller. *IFAC Workshop on MPC Oxford*. (1988): 23-29.
- [21] M. Chaudhary. *Real Time Optimization of Chemical Processes*. Master thesis, Curtin University of Technology, Australia. 2009.
- [22] J. Ren, S. Tan, L. Dong, S. He, and X. Ji. Optimization of the reflux ratio for a stage Distillation Column based on an improved particle swarm algorithm. *Journal of Chemical and Process Engineering, Polish Academy of Sciences*. 31. (2010): 15-24.
- [23] T. Edgar, D. Himmelblau, and L. Lasdon. *Optimization of chemical processes*. McGraw-Hill Science/Engineering/Math. second ed.. 2001.
- [24] L. Wang. *Model Predictive Control System Design and Implementation Using MATLAB*. Springer. 2009.

- [25] T. Boom and T. Backx. *Model Predictive Control*. Lecture Notes for the MPC DISC Course, Delft University of Technology, The Netherlands. 1999. [Online] Available at <http://lcewww.et.tudelft.nl/~discmpc/>.
- [26] C. Brosilow and B. Joseph. *Techniques of Model-Based Control*. Prentice Hall PTR. 2002.
- [27] S. Skogestad. *Distillation research and models*. [Online] Available at <http://www.nt.ntnu.no/users/skoge/distillation/>.
- [28] S. Skogestad and I. Postlethwaite. *Multivariable Feedback Control: Analysis and Design*. John Wiley and Sons. 2005.
- [29] M. Grant, S. Boyd, and Y. Ye. *cvx: Matlab software for disciplined convex programming*. Stanford University. 2008. [Online] Available at <http://www.stanford.edu/~boyd/cvx>.
- [30] D. Dougherty and D. Cooper. A practical multiple model adaptive strategy for multivariable Model Predictive Control. *Control Engineering Practice*. 11. (2003): 649-664.
- [31] C. Porfirio, E. A. Neto, and D. Odloak. Multi-model Predictive Control of an industrial C3/C4 splitter. *Control Engineering Practice*. 11. (2003): 765-779.
- [32] L. Ciprian, U. Andreea, P. Dumitru, and F. Cristian. Stable algorithms switching for multiple models control systems. *WSEAS Transactions on Systems*. 8. 4. (2009): 451-460.
- [33] Z. Tian and K. Hoo. Transition control using a state-shared model approach. *Computers and Chemical Engineering*. 27. (2003): 1641-1656.
- [34] Z. Tian. *Multiple Model Predictive Control framework for multi-input multi-output continuous processes*. PhD thesis. Texas Tech University. 2003.

## Appendix

### Dynamic Equations to describe the Propylene Splitter

The assumptions and the dynamic equations to describe the mathematical model of a distillation column are as follows [27].

- *Assumptions*

Constant relative volatility

$$\alpha = \frac{y_L/x_L}{y_H/x_H} = \frac{y_L/y_H}{x_L/x_H} \quad (1)$$

( $L$  - the light component (propylene);  $H$  - the heavy component (propane))

Constant molar flows: at steady state

$$L_i = L_{i+1}; \quad V_i = V_{i+1} \quad (2)$$

No vapor holdup (immediate vapor response,  $dV_{\text{top}} = dV_{\text{btm}}$ ).

Liquid holdup  $M_i$  constant (immediate liquid response,  $dL_{\text{top}} = dL_{\text{btm}}$ ).

Vapor liquid equilibrium (VLE) and perfect mixing on each stage.

Perfect level control in accumulator and column base, pressure constant.

- *Dynamic Equations*

The states are the mole fractions of the light component (propylene)  $x_i$  and the liquid holdup  $M_i$  – a total of  $2N_T$  states.

The vapor-liquid equilibrium relationship can be used

$i = 1 : N_T - 1$ :

$$y_i = \frac{\alpha x_i}{1 + (\alpha - 1)x_i} \quad (3)$$

$x_i$ ,  $y_i$  are state (liquid composition), output (vapor composition) at the tray  $i$ ;  $\alpha$  is the relative volatility between light and heavy component.

The vapor flow's equation and molar flows through all trays are assumed to constant in all states.

$i = 1 : N_T - 1$ :

$$V_i = V_b \quad (4)$$

( $V_b$  is the feed at the bottom tray).

$i = N_f : N_T - 1$ :

$$V_i = V_i + (1 - q_f)F \quad (5)$$

Liquid flow's equation and the linearized tray hydraulics with time constant  $\tau$ , also includes coefficient  $\lambda$  for effect of vapor flow ("K2-effect").

$i = 2 : N_f$ :

$$L_i = L_{0b} + (M_i - M_{0i}/\tau) + \lambda(V_{i-1} - V_0) \quad (6)$$

$i = N_f + 1 : N_T - 1$ :

$$L_i = L_0 + (M_i - M_{0i}/\tau) + \lambda(V_{i-1} - V_{0t}) \quad (7)$$

$$L_{N_T} = L_T \quad (8)$$

Time derivatives from material balances for (1) total holdup and (2) component holdup in each stage of the column as follows.

$i = 2 : N_T - 1$ :

$$dM_i/dt = L_{i+1} - L_i + V_{i-1} - V_i \quad (9)$$

$$d(M_i x_i)/dt = L_{i+1} x_{i+1} - L_i x_i + V_{i-1} y_{i-1} - V_i y_i \quad (10)$$

Correction for feed at the feed stage. The feed is assumed to be mixed into the feed stage

$$dM_{N_f}/dt = dM_{N_f}/dt + F \quad (11)$$

$$d(M_{N_f} x_{N_f})/dt = d(M_{N_f} x_{N_f})/dt + F z_f \quad (12)$$

Reboiler (assumed to be an equilibrium stage)

$$dM_1/dt = L_2 - V_1 - B \quad (13)$$

$$dM_1 x/dt = L_2 x_2 - V_1 y_1 - B x_1 \quad (14)$$

Total condenser (no equilibrium stage)

$$dM_{N_T}/dt = V_{N_T-1} - L_{N_T} - D \quad (15)$$

$$d(M_{N_T} x_{N_T})/dt = V_{N_T-1} y_{N_T-1} - L_{N_T} x_{N_T} - D x_{N_T} \quad (16)$$

Compute the derivative for the mole fractions from  $d(Mx) = x dM + M dx$

$i = 1 : N_T$ :

$$dx_i/dt = (d(M_i x_i)/dt - x_i dM_i/dt)/M_i \quad (17)$$

All the equations above are in the file **colamod.m** as in disk recording. The model is non-linear with  $2N_T$  states. The model has 4 manipulated inputs including  $[L_T, V_T, D, B]$ ; 2 disturbances  $[F, X_f]$  and 2 outputs  $[X_d, X_b]$ . We will use  $D$  to control the level  $M_D$  and  $B$  to control the level  $M_B$ . This is done by two proportional controllers with both gains equal to 10 (see the file **colarv.m** in disk recording).



## BIOGRAPHY

Phuc Xuan Dang was born in 1985 at Thaibinh, Vietnam. He received his Bachelor's degree in Industrial Automation from Faculty of Electrical Engineering, Hanoi University of Technology, Vietnam, in August 2008. He has been granted a scholarship by the AUN/SEED-Net ([www.seed-net.org](http://www.seed-net.org)) to pursue his Master's degree in Electrical Engineering at Chulalongkorn University, Thailand, since June 2009. He has studied a Master's degree program with a focus on Control Systems at the Department of Electrical Engineering, Faculty of Engineering, Chulalongkorn University from June 2009 to May 2011. His research interest includes model predictive control, real time optimization, distillation column.

### List of Publications

1. P. X. Dang, D. Banjerdpongchai, "Design of Integrated Real Time Optimization and Model Predictive Control for Distillation Column", in *Proceedings of the 8th Asian Control Conference*, Splendor Hotel, Kaohsiung, Taiwan, May 16-18, 2011.

ศูนย์วิทยทรัพยากร  
จุฬาลงกรณ์มหาวิทยาลัย